



2015

# 14th Oxford Summer School on Neutron Scattering

## Answer Book

A) Coherent and Incoherent Scattering	1
B) Time-of-flight Powder Diffraction	4
C) Single Crystal Diffraction	9
D) Incoherent Inelastic Scattering	14
E) Coherent Inelastic Scattering	19
F) High Resolution Spectroscopy	22
G) Small Angle Scattering	26
H) Reflectometry	30
I) Polarized Neutrons	36
J) Spin-Echo Small Angle Neutron Scattering	39
K) Magnetic Scattering	42
L) Chemical applications	46
M) Biological Applications	48
N) Disordered Materials Diffraction	50

The school is supported by:



Science & Technology Facilities Council



<http://www.oxfordneutronschool.org>

## A. Coherent and Incoherent Scattering

### **A1**

(1) Hydrogen.  $b_{\text{coh}}$  is derived by averaging the scattering length over the states with parallel and antiparallel neutron–nucleus spin states, Eq. (B2),

$$b_{\text{coh}} = \bar{b} = w^+ b^+ + w^- b^-$$

The weights are given by Eq. (A1):  $w^+ = (I+1)/(2I+1)$  and  $w^- = I/(2I+1)$ . Setting  $I = 1/2$  we have  $w^+ = 3/4$  and  $w^- = 1/4$ . From Table A1,

$$b_{\text{coh}} = \frac{3}{4}(10.85) + \frac{1}{4}(-47.5) \text{ fm}$$

$$\equiv -3.74 \text{ fm}$$

The coherent scattering cross section is given by Eq. (A3),

$$\sigma_{\text{coh}} = 4\pi b_{\text{coh}}^2$$

$$\equiv 1.75 \text{ b} \quad (1 \text{ b} = 10^{-28} \text{ m}^2)$$

The total cross section is obtained by summing the weighted values of the spin states of the combined nucleus-neutron system, Eq. (A4):

$$\sigma_{\text{tot}} = 4\pi\{w^+(b^+)^2 + w^-(b^-)^2\}$$

$$\equiv 81.6 \text{ b}$$

Finally, the incoherent scattering cross section is the difference between  $\sigma_{\text{tot}}$  and  $\sigma_{\text{coh}}$ ,

$$\sigma_{\text{inc}} = \sigma_{\text{tot}} - \sigma_{\text{coh}}$$

$$\equiv 79.9 \text{ b}$$

(1) Deuterium. For  $I = 1$  we have from Eq. (A1),  $w^+ = 2/3$  and  $w^- = 1/3$ . From the data in Table A1, and the formulae above,

$$b_{\text{coh}} = 6.67 \text{ fm}$$

$$\sigma_{\text{coh}} = 5.6 \text{ b}$$

$$\underline{\sigma_{\text{tot}} = 7.6 \text{ b}}$$

$$\underline{\sigma_{\text{inc}} = 2.0 \text{ b}}$$

## A2

In this example the incoherent scattering is mainly isotopic in origin, but there is a small contribution from the spin.

The coherent scattering length is the weighted average of the scattering lengths of the different isotopes, Eq. (A2):

$$b_{\text{coh}} = \bar{b} = \sum_r c_r (w_r^+ b_r^+ + w_r^- b_r^-)$$

Using Table A1a below we have:

$$\underline{b_{\text{coh}} = 10.34 \text{ fm}}$$

The coherent scattering cross section is given by Eq. (A3),

$$\sigma_{\text{coh}} = 4\pi b_{\text{coh}}^2 = 4\pi \bar{b}^2$$

$$\underline{= 13.43 \text{ b}}$$

The total scattering cross section is given by Eq. (A4),

$$\sigma_{\text{tot}} = 4\pi \sum_r c_r \{w_r^+(b_r^+)^2 + w_r^-(b_r^-)^2\}$$

where,

$$w_r^+ = \frac{I_r+1}{2I_r+1} \text{ and } w_r^- = \frac{I_r}{2I_r+1}$$

Hence,

$$\underline{\sigma_{\text{tot}} = 18.50 \text{ b}}$$

Finally, from Eq. (A5),  $\sigma_{\text{inc}} = \sigma_{\text{tot}} - \sigma_{\text{coh}}$ , we find that

$$\underline{\sigma_{\text{inc}} = 5.09 \text{ b}}$$

Table A.2a.

isotope, $r$	spin $I_r$	$c_r (w_r^+ b_r^+)$ (fm)	$c_r (w_r^- b_r^-)$ (fm)	$c_r w_r^+ (b_r^+)^2$ (b)	$c_r w_r^- (b_r^-)^2$ (b)
58	0	9.835	0	1.416	0
60	0	0.73	0	0.020	0
61	3/2	0.031	0.052	0.132	0.595
62	0	-0.31	0	0.027	0
64	0	- 0.004	0	0.000	0

## **B. Time-of-Flight Powder Diffraction**

### **B1.**

(a) The expression

$$t = \left( \frac{m_n}{h} \right) \lambda L$$

follows from the relations

$$L = vt$$

$$\lambda = \frac{h}{m_n v}$$

Where  $v$  is the neutron velocity.

From the values of  $h$  and  $m_n$  on page 1 we get

$$t (\mu\text{secs}) = 251.9 \times \lambda (\text{\AA}) \times L (\text{m}) \quad (\text{B1a})$$

(b) In Bragg scattering from lattice planes  $HKL$  of spacing  $d_{HKL}$  the wavelength of the scattered radiation is given by

$$\lambda = 2d_{HKL} \sin\theta \quad (\text{B2a})$$

where  $2\theta$  is the scattering angle. Putting  $L = 100$  m into eqn. (B1a) and  $\theta = 85^\circ$  into eqn. (B2a) gives

$$t (\mu\text{secs}) = 5.019 \times 10^4 d_{HKL} (\text{\AA}) \quad (\text{B3a})$$

Perovskite has a primitive cubic lattice, so that the first three Bragg reflections (corresponding to the longest times-of-flight) are  $100$ ,  $110$  and  $111$ . The d-spacing is related to the lattice constant  $a_0$  by

$$d_{HKL} = a_0 (H^2 + K^2 + L^2)^{-1/2} \quad (\text{B4a})$$

Therefore;  $d_{100} = 3.84$  Å,  $d_{110} = 2.72$  Å and  $d_{111} = 2.22$  Å.

Substituting into eqn. (B3a) we find that

$$t_{100} = 193 \text{ ms}, t_{110} = 137 \text{ ms} \text{ and } t_{111} = 111 \text{ ms.}$$

(c) Combining eqns. (B3a) and (B4a) gives:

$$t \propto (H^2 + K^2 + L^2)^{-1/2} \quad (\text{B5a})$$

## B2.

(a) The *Structure Factor*  $F_{HKL}$ , or the amplitude of the scattering into the  $HKL$  Bragg reflection by the atoms in one unit cell, is given by:

$$F_{(HKL)} = \sum_n b_n \exp [i2\pi(Hx_n + Ky_n + Lz_n)] \quad (\text{B6a})$$

Here  $b_n$  is the scattering length of the  $n^{\text{th}}$  nucleus in the cell,  $x_n y_n z_n$  are its fractional coordinates. The sum is taken over all atoms in the unit cell.

In the diamond structure of silicon there is a basis of two silicon atoms at

$0,0,0$  and  $\frac{1}{4},\frac{1}{4},\frac{1}{4}$

and this basis is distributed at each of the face-centred-cubic lattice points:

$0,0,0; \quad \frac{1}{2},\frac{1}{2},0; \quad \frac{1}{2},0,\frac{1}{2}; \quad 0,\frac{1}{2},\frac{1}{2}$

There are therefore 8 atoms in the unit cell, with fractional coordinates

$(0,0,0; \quad \frac{1}{2},\frac{1}{2},0; \quad \frac{1}{2},0,\frac{1}{2}; \quad 0,\frac{1}{2},\frac{1}{2})$  for  $n = 1$  to 4

and

$\frac{1}{4},\frac{1}{4},\frac{1}{4} + (0,0,0; \quad \frac{1}{2},\frac{1}{2},0; \quad \frac{1}{2},0,\frac{1}{2}; \quad 0,\frac{1}{2},\frac{1}{2})$  for  $n = 5$  to 8

Inserting these coordinates into eqn. (B6a) gives:

$$\begin{aligned} F_{(HKL)} = b_{Si} & \left\{ 1 + e^{i\pi(H+K)} + e^{i\pi(H+L)} + e^{i\pi(K+L)} \right. \\ & + e^{i\frac{\pi}{2}(H+K+L)} + e^{i\frac{\pi}{2}(3H+3K+L)} \\ & \left. + e^{i\frac{\pi}{2}(3H+K+3L)} + e^{i\frac{\pi}{2}(H+3K+3L)} \right\} \end{aligned}$$

This then can be written,

$$\begin{aligned} F_{(HKL)} = b_{Si} & \left\{ 1 + e^{i\pi(H+K)} + e^{i\pi(H+L)} + e^{i\pi(K+L)} \right\} \\ & \times \left\{ 1 + e^{i\frac{\pi}{2}(H+K+L)} \right\} \quad (\text{B7a}) \end{aligned}$$

If  $H, K$  and  $L$  are mixed odd or even numbers, then the term in the first {} bracket is zero. (2 out of the 3 exponential terms is -1, the third is +1)

(b) A further restriction on the indices of the Bragg reflections is imposed by the second bracket {} in eqn. (B7a). If  $\frac{1}{2}(H+K+L)$  is even, this bracket is equal to 2; if  $\frac{1}{2}(H+K+L)$  is odd, the bracket is zero.

(c)

(i) The possible values of  $HKL$  for the f.c.c. lattice are shown in Table C.1a.

**Table B1a**

*Sums of three squared integers/ Miller indices.*

$H^2+K^2+L^2 / HKL$	$H^2+K^2+L^2 / HKL$	$H^2+K^2+L^2 / HKL$	$H^2+K^2+L^2 / HKL$
3* 111	12* 222	21	32* 440
4* 200	13	22	33
5	14	24* 422	34
6	16* 400	25	35* 531
8* 220	17	26	36* 600/442
9	18	27* 511/333	37
10	19* 331	29	38
11* 311	20* 420	30	40* 620

(ii) The forbidden reflections are: 200, 222, 420, 600/442

(iii) The overlapping reflection is: 511/333

(d) Putting  $L = 96.8$  m into eqn. (B1a) and  $\theta = 45.4^\circ$  into eqn. (B2a) gives

$$t \text{ (ms)} = 34.724 d_{HKL} \text{ (\AA)} \quad (\text{B8a})$$

111 is the Bragg peak with the longest flight time. The next peak is 220 (200 is forbidden). Thus 220 is peak no 2 in Figure B1. Using the information in section (c) the remaining peaks are readily indexed (see Table B2a below).

**Table B2a**

	time of flight (ms)	<i>d</i> -spacing	<i>HKL</i>	$H^2+K^2+L^2$	$a_0 = d_{HKL} \times \sqrt{H^2 + K^2 + L^2}$
1	109.232	3.146	111	3	5.44903
2	66.912	1.927	220	8	5.45038
3	57.066	1.643	311	11	5.44921
4	47.320	1.363	400	16	5.45200
5	43.424	1.251	331	19	5.45298
6	38.636	1.113	422	24	5.45256
7	36.426	1.049	511/333	27	5.45076
8	33.457	0.964	440	32	5.45321
9	31.991	0.921	531	35	5.44871
10	29.923	0.862	620	40	5.45177

Taking the mean of the lattice constant calculated from the peaks – excluding the first peak – we get for the lattice constant of Si.

$$a_0 = 5.45106 \text{ \AA}$$

The calculation from the first peak is slightly out due to a higher order term in the time-of-flight to d-spacing conversion. This comes about due to the fact that the total flight path of the neutron is related to the wavelength. In general, short wavelength neutrons will penetrate further into the sample than long wavelength neutrons, and so the total flight path therefore becomes a function of both  $2\theta$  and  $\lambda$ .

Observed times-of-flight of reflections may be noticeably different from those expected from the expression C8a, especially at longer d-spacings (which are measured with neutrons of longer wavelength, where absorption is greater). Empirically, it is found that a quadratic dependence provides a good description of the shifts in the reflection positions.

In GSAS for example, each diffraction bank is characterised by three constants. DIFC (which is the constant  $251.9 \times L \sin \theta$  that we calculated above), DIFA – proportional to  $d^2$  and ZERO, which accounts for any offset in the measured timing of the data acquisition system. Altogether this gives

$$t (\mu\text{secs}) = 251.9 \times \text{DIFC } d_{HKL} (\text{\AA}) + \text{DIFA } d_{HKL}^2 (\text{\AA}^2) + \text{ZERO} \quad (\text{C9a})$$

These diffractometer constants are fixed by the instrument parameters, and should not be refined.

### B3.

- (a) Bragg's Law is  $\lambda = 2d \sin \theta$

Differentiating with d with respect to theta

$$\frac{\Delta d}{\Delta \theta} = \frac{\lambda \cos \theta}{2 \sin^2 \theta}$$
$$\Rightarrow \frac{\Delta d}{d} = \cot \theta \Delta \theta$$

- (b) since  $\lambda = h t / m L$  we can substitute this into Bragg's Law to give

$$d = \frac{ht}{2m_n L \sin \theta}$$

Therefore, since d is linear in the distance L, the relative uncertainties in d and L will be equal.

- (c)  $\Delta L = 0.02$  m, therefore:

- i)  $L = 10$  m for a d-spacing resolution of  $2 \times 10^{-3}$
- ii)  $L = 40$  m for a d-spacing resolution of  $5 \times 10^{-4}$

POLARIS and HRPD roughly follow these lengths. The actual lengths are longer – esp. for HRPD – due to other contributions to the d-spacing resolution being added in quadrature. The most important of these is the time-resolution of the moderator.

## **C. Single-Crystal Diffraction**

### **C1.**

(i) From the relation  $\lambda = h/(m_n v)$  we get

$$\lambda (\text{\AA}) = 3.956 / v (\text{km s}^{-1}).$$

Putting  $v = 2.20 \text{ km s}^{-1}$  gives  $\lambda = 1.8 \text{ \AA}$ .

(ii) Similarly from  $E = \frac{1}{2}m_n v^2$  we obtain  $E = 25.3 \text{ meV}$ .

(iii) The X-ray energy is given by:

$$E_{X-Ray} = h\nu = \frac{hc}{\lambda}$$

with  $\nu$  the frequency of the X-rays and  $c$  the velocity of light.  
Putting  $c = 3 \times 10^8 \text{ ms}^{-1}$  gives

$$E = 6.9 \text{ keV}$$

(iv) The velocity of a neutron with this energy is

$$v = \left( \frac{2E}{m_n} \right)^{\frac{1}{2}}$$

therefore,  $v = 1150 \text{ km s}^{-1}$

*We see then that thermal neutrons have both wavelengths suitable for studying atomic structures in the 1-100 \text{\AA} range and energies suitable for studying coherent excitations (such as phonons or magnons) in the meV range. (Fast neutrons have too short a wavelength and are too energetic for either purpose.)*

## C2

(i). The wavelength of the reflected beam is

$$\lambda = 2d_{111} \sin\theta$$

where  $d_{111} = a_0 / \sqrt{3}$ . Thus  $\sin\theta = 1.8 / 5.7$  and the scattering angle is

$$2\theta = 36.8^\circ$$

(ii). The wavelength spread is derived by differentiating Bragg's with respect to  $\theta$

$$\frac{\Delta\lambda}{\lambda} = \cot\theta \cdot \Delta\theta$$

Putting  $\Delta\theta = 0.2^\circ$  ( $= 0.0035$  rad.) gives  $\frac{\Delta\lambda}{\lambda} = 0.0105$ , so that for  $\lambda = 1.8 \text{ \AA}$  we get

$$\Delta\lambda = \pm 0.018 \text{ \AA}$$

*Note that this spread of wavelengths is much larger than the natural width of characteristic X-ray lines, and so Bragg peaks obtained with neutrons will not be as sharp as X-ray peaks.*

### C3

Figure C1a shows the reciprocal lattice in the  $\mathbf{a}^*\mathbf{b}^*$  plane, together with the Ewald circles passing through the reflections (630) and (360).

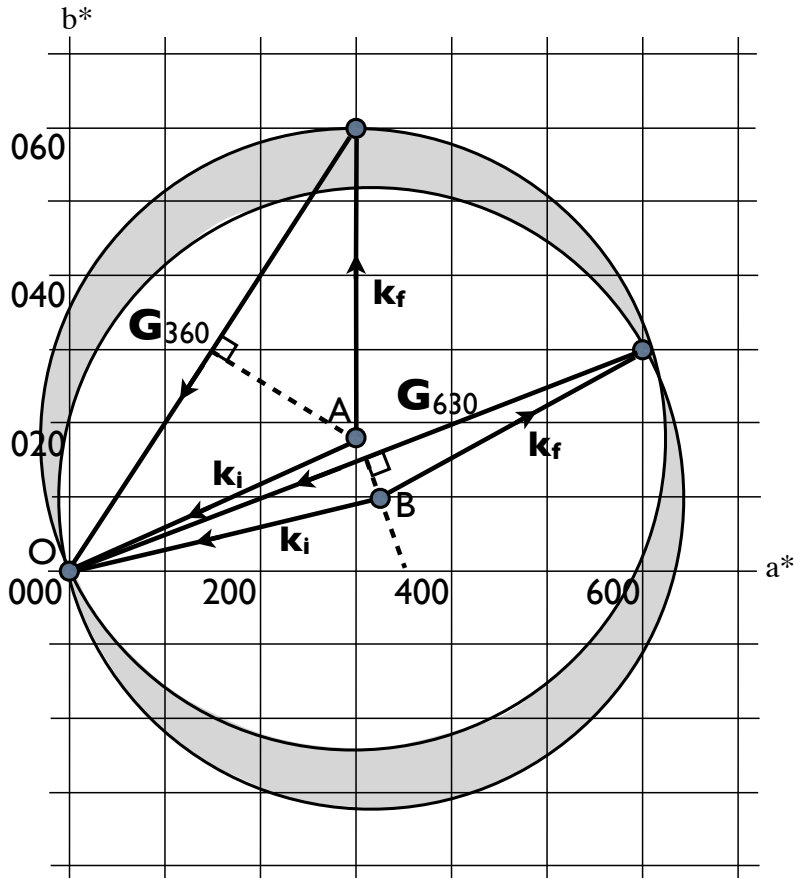


**Figure C1a.** The Ewald circles for the (630) and (360) reflections. A is the centre of the circle for (360) and B is the centre of the circle for (630).

We can consider the crystal to be stationary and the incident beam to turn between the directions  $\mathbf{AO} \rightarrow$  and  $\mathbf{BO} \rightarrow$  in the Figure. During this rotation the area swept out in reciprocal space is the shaded region. The number of reciprocal lattice points in this region, i.e. the number of Bragg reflections, is approximately 13.

### C4

Figure C2a shows the Ewald circles drawn for the two extreme wavelengths. The observable reflections are those lying in the shaded area lying between the two circles. For a primitive unit cell there are no systematically absent reflections, and so the number of possible reflections is about 40.

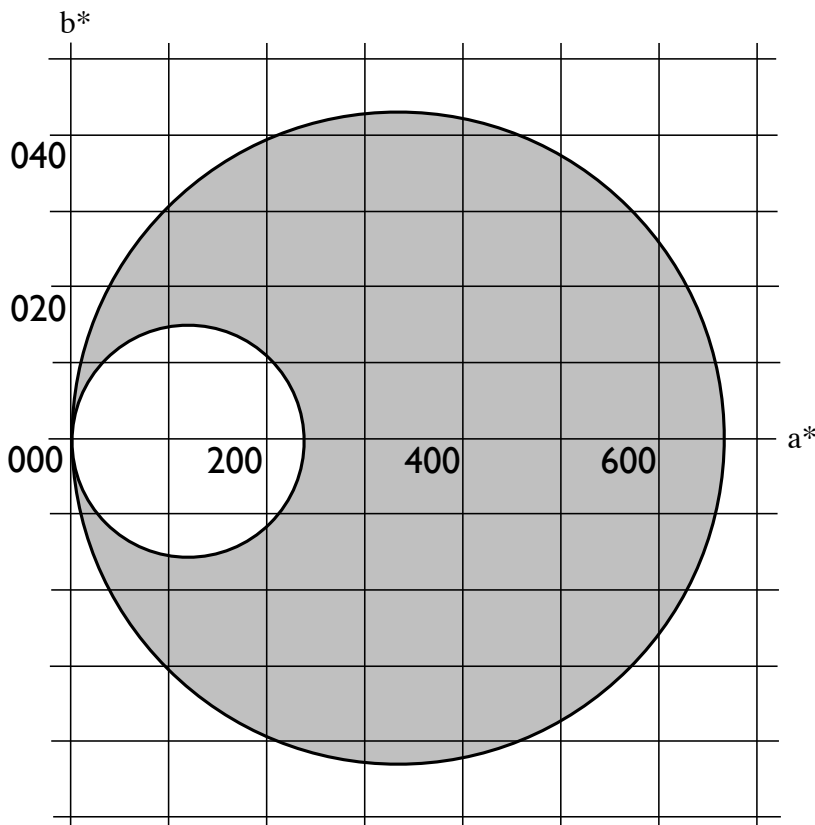


**Figure C2a** The Ewald construction showing the reflection circles for the minimum wavelength (maximum radius) and the maximum wavelength (minimum radius).

## C5

- (i) The intensity of the  $(00L)$  reflection is proportional to the square of the structure factor;

$$F_{(HKL)} = \sum_n b_n \exp [i2\pi(Hx_n + Ky_n + Lz_n)]$$

Where the sum is over the atoms in the unit cell of the crystal.

Therefore the structure factor for the  $(00L)$  reflection is;

$$\begin{aligned} F_{(00L)} &= b_{Ba} \exp [0] + b_{Ti} \exp [i\pi L] + b_O \exp [0] + 2b_O \exp [i\pi L] \\ I_{(00L)} &= b_{Ba} + (-1)^L b_{Ti} + [1 + 2(-1)^L] b_O \quad \text{is} \end{aligned}$$

therefore proportional to the square of this expression.

- (ii) For the  $(005)$  reflection, we can substitute the scattering lengths to find

$$F_{(005)} = 5.25 + 3.30 - 5.81 = 2.74$$

and therefore

$$I_{(005)} \propto |F_{(005)}|^2 = 7.51$$

For the distorted case we have the structure factor;

$$\begin{aligned} F_{(005)}^\delta &= \sum_n b_n \exp[i2\pi L(z_n + \delta_n)] \\ &= \sum_n b_n \exp[i2\pi Lz_n] \exp[i2\pi L\delta_n] \end{aligned}$$

where  $\delta_n = 0$  for the Ba atoms,  $+\delta$  for the Ti atoms,  $-\delta$  for the O atoms, and  $L = 5$ . Writing this out in full as before, we have

$$F_{(005)}^\delta = b_{Ba} - b_{Ti} \exp(i10\pi\delta) - b_O \exp(-i10\pi\delta)$$

Assuming small displacements, we can expand the exponential terms to first order, giving

$$\begin{aligned} F_{(005)}^\delta &= b_{Ba} - b_{Ti}(1 + i10\pi\delta) - b_O(1 - i10\pi\delta) \\ &= 2.74 + i286\delta \end{aligned}$$

and therefore

$$\begin{aligned} I_{(005)}^\delta &\propto |F_{(005)}^\delta|^2 = (2.74 + i286\delta)(2.74 - i286\delta) \\ &= 7.51 + 81796\delta^2 \end{aligned}$$

Since the Bragg peak intensity increases by 74% due to the distortion, we can write

$$\begin{aligned} \frac{I_{(005)}^\delta}{I_{(005)}} &= \frac{7.51 + 81796\delta^2}{7.51} = 1.74 \\ &\Rightarrow 10891\delta^2 = 0.74 \\ &\Rightarrow \delta = 0.0083 \end{aligned}$$

[remember that this is the distortion expressed as a fraction of the lattice constant]

(iii) For the X-ray case, the structure factors are proportional to

$$\begin{aligned} F_{(005)} &= 56 - 22 - 8 = 26 \\ F_{(005)}^\delta &= 56 - 22(1 + i10\pi\delta) - 8(1 - i10\pi\delta) \\ &= 26 + i440\delta \end{aligned}$$

so now the ratio of the intensities becomes

$$\begin{aligned} \frac{I_{(005)}^\delta}{I_{(005)}} &= \frac{676 + 193600\delta^2}{676} \\ &= 1 + 286 \times (0.0083)^2 \\ &= 1.019 \end{aligned}$$

So the increase in intensity of the (005) reflection is only 1.9% compared to the undistorted structure. This is due to a number of factors, including the greater sensitivity of neutrons to oxygen atoms, the negative scattering amplitude of the Ti, and the fact that the X-ray structure factor is dominated by the Ba atom, which does not move under the distortion.

## **D. Incoherent Inelastic Scattering (with a Pulsed Neutron Spectrometer)**

### **D1.**

(i) The elastic peak in Figure D3a occurs at the time of flight  $t \approx 63.7$  ms. The total flight path is  $36.41\text{m} + 1.45\text{m} = 37.86\text{m}$ , and so the neutron velocity is  $v_n = 594.3$  m/s.

The energy selected by the analyser crystal is

$$E_n = \frac{1}{2} m_n v_n^2 = \mathbf{1.843 \text{ meV}}$$

(ii) Bragg's Law is  $\lambda = 2d_{002}\sin\theta$ . First, we need to calculate the wavelength of the neutrons. Using

$$\lambda_n v_n = h/m_n$$

$\lambda_n = 6.68\text{\AA}$ , such that  $\theta = 85.6^\circ$

(iii) The advantage of using a high take-off angle  $2\theta \approx 170^\circ$  is that the wavelength band reflected by the analyser is then relatively small [such that the contribution to the resolution ( $\cot\theta \times \Delta\theta$ ) tends to zero].

### **D2.**

(i) Figure D2 shows the monitor spectrum after the second chopper. The fastest neutron enters at 52.2ms and the slowest at 72.2ms. The distance they have to travel from the moderator is  $36.41 - 0.355 = 36.055$  m. Thus the chopper is letting through neutrons travelling at speeds between 499.4 m/s and 690.7 m/s.

Using  $\lambda_n = h/m_n v_n$  gives an incoming **wavelength band of  $5.73\text{\AA}$  and  $7.92\text{\AA}$** .

(ii) The energy of these neutrons is then:

$$E_n = \frac{1}{2} m_n v_n^2 = 2.496 \text{ meV and } 1.302 \text{ meV}$$

We know that the energy selected by the analyser crystal is 1.843 meV, so then the energy transfer possible will be:

$$\Delta E_{\max} = E_i - E_f = 2.496 - 1.845 = \mathbf{0.651 \text{ meV}}$$

$$\Delta E_{\min} = E_i - E_f = 1.302 - 1.845 = \mathbf{-0.543 \text{ meV}}$$

(iii) Neutrons that have gained energy will arrive at the detector at a later time than the elastically scattered neutrons, whereas the neutrons that have lost energy will arrive at the detector at an earlier time. This might sound counterintuitive but it is because of the inverted geometry of the instrument.

So for example, the fastest neutron of wavelength 5.73 Å and velocity 690.7m/s will arrive at the sample at 52.71 ms. If it is reflected by the analyser it means that upon interaction with the sample it has changed its speed to 594.3 m/s, ie. it has slowed down. Thus it will take 2.44 ms to travel from the sample to the detector. So this neutron will reach the detector at  $t = 52.71 + 2.44 = 55.15$  ms (earlier than the elastically scattered neutrons which arrive at 63.7 ms).

In a direct geometry instrument the opposite happens, neutrons that have gained energy will arrive at the detector earlier than the elastically scattered neutrons, and neutrons that have lost energy will arrive later.

So the inelastic peaks in Figure D3b are at  **$t = 60.95 \text{ ms for the energy loss and at 66.89 ms for the energy gain.}$**

(iv) The neutron that has gained energy must have arrived at the sample at  $66.89 - 2.44 = 64.45$  ms, with a velocity of  $v = 36.41 \text{ m}/64.45 \text{ ms} = 564.93 \text{ m/s}$ , i.e an energy of  $E = 1.666 \text{ meV}$ .

The neutron that has lost energy must have arrived at the sample at  $60.95 - 2.44 = 58.51$  ms, with a velocity of  $v = 36.41 \text{ m}/64.45 \text{ ms} = 622.29 \text{ m/s}$ , i.e an energy of  $E = 2.021 \text{ meV}$ .

So the energy transfer is  **$\pm 0.178 \text{ meV}$** .

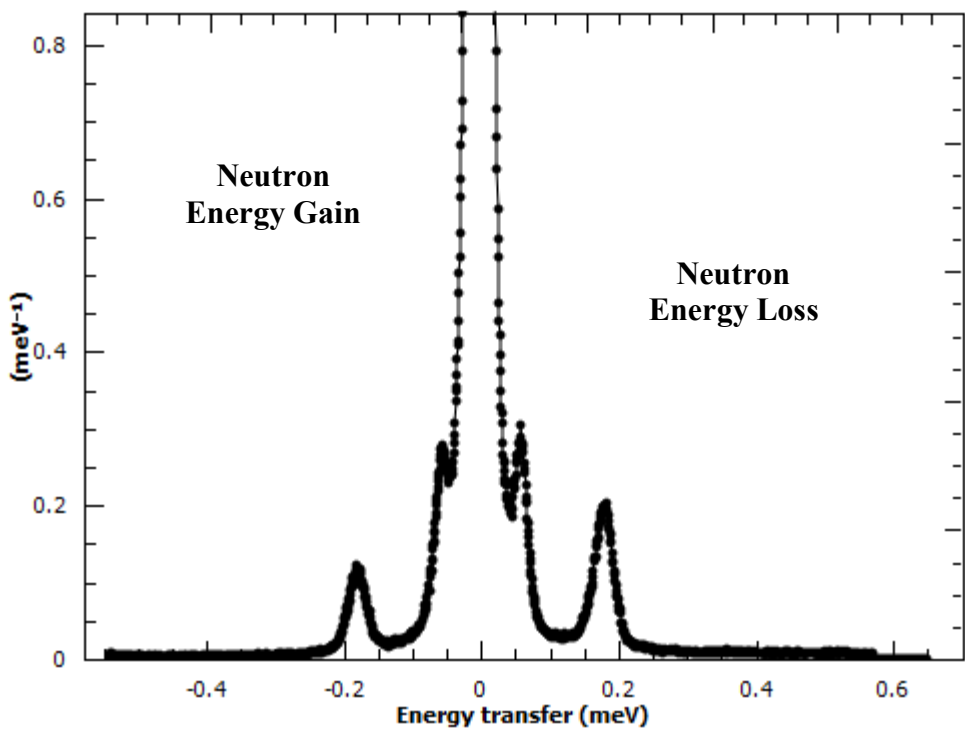


**Figure D1a.** IRIS spectrum of an ionic liquid at 4K (same as Figure D3)

(v) The intensity is influenced by the Bose factor  $n(E)$  which gives the number of phonons which exist at a given energy  $E$  and temperature  $T$ :

$$n(E) = \frac{1}{\exp\left(\frac{E}{k_B T}\right) - 1}$$

For neutron-energy loss the intensity is proportional to  $[1 + n(E)]$ , whereas for neutron-energy gain it is proportional to  $n(E)$ . At low temperatures  $n(E)$  tends to zero and only scattering with neutron energy loss ('down scattering') is possible. There is always a greater possibility, at any temperature, that neutrons will be scattered with energy loss.

In this case the Bose-factor **n(E) = 1.45** (assuming the sample is at 4 K) resulting in a ratio of peak intensities of 0.6 (energy gain peak / energy loss peak)

## D3

(i) The first chopper is used to select the wavelength band and the second to remove frame overlap.

(ii) To look at larger energy transfers we would have to open up our incoming wavelength band. There are several ways we could do this:

a. Run the choppers at a slower speed (multiple of 50Hz) to open up the window. For example we could use 25Hz, but we would have to count twice as long.

b. Run the choppers at the same speed but phase them to let the higher energy neutrons in and use the PG004 (higher energy reflection) reflection from the analyser crystals. When you use higher energy neutrons you need to consider two extra things – a worsening of the resolution and possibly a change in incident neutron flux. On IRIS the resolution changes from 17.5ueV to 54.5ueV going from 002 to 004, and the loss in flux is around 20%.

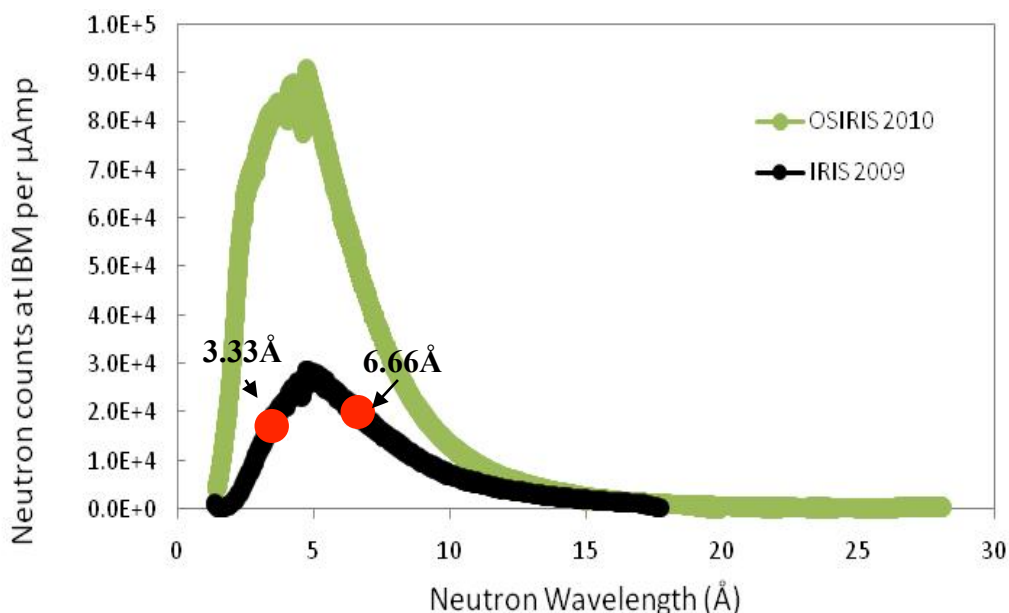


**Figure D2a.** Incident monitor spectrum from the ISIS TS1 hydrogen moderator showing the distribution of neutrons for IRIS (and OSIRIS) as a function of incoming wavelength.

Case (a)

Running a symmetric window at 25Hz gives an opening of 40ms and we know that the centre is at 63.7ms which is for the elastically scattered neutrons at 6.66 Å. Thus we want the detector window to be 43.7ms to 83.7.

	Min	Elastic	Max
Tof (ms) at detector 37.86m	43.7	63.7	83.7
Wavelength (Å)	4.57	6.66	8.74
Energy (meV)	3.92	1.84	1.07
$\Delta E$ (meV)	2.08		-0.77

The choppers would then need to be set at opening and closing times of:

	Min	Max
Tof (ms) at first chopper at 6.3m	7272	13928
Tof (ms) at second chopper at 10m	11542	22108

### Case (b)

Choppers should be run at 50Hz and the time window at the detector is still 20ms but we need to open the choppers at different times to let different energy neutrons through. We had calculated before that the 004 reflection is for 3.33 Å neutrons that would be scattered elastically and arrive at the detector at 31.87ms. So, following a similar procedure:

	Min	Elastic	Max
Tof (ms) at detector 37.86m	22.0	31.87	42.0
Wavelength (Å)	2.30	3.33	4.39
Energy (meV)	15.48	7.38	4.25
$\Delta E$ (meV)	8.1		-3.13

The choppers would then need to be set at opening and closing times of:

	Min	Max
Tof (ms) at first chopper at 6.3m	3663	6992
Tof (ms) at second chopper at 10m	5814	11099

(iii) One could choose a different analyser crystal that could reflect at difference d-spacings. In fact on the empty side of the instrument we have a Mica crystal bank that allows us to look at the 002, 004 and 006 reflections: which are at 0.207meV, 0.826meV and 1.86meV. But here you have to consider the change in the resolution and also the intensity (incident flux due to change in wavelength PLUS reflectivity of the crystals).

	Energy	$\Delta E$ (meV)	$E$ Res(ueV)	Intensity
Mi002	0.207	+/-0.022	1.2	0.04
Mi004	0.826	+/- 0.2	4.5	0.15
Mi006	1.86	+/- 0.5	11	0.40

## E. Coherent Inelastic Scattering (with a Three-Axis Spectrometer)

### **E1.**

The allowed points have  $HKL$  indices, which are all odd or all even. See Figure E1a.

### **E2.**

The relation between neutron energy  $E$  and neutron wave number  $k$  is

$$E \text{ (meV)} = 2.072 [k \text{ (\AA}^{-1})]^2$$

Putting  $E_i^{\min} = 3 \text{ meV}$  and  $E_i^{\max} = 14 \text{ meV}$  gives

$$k_i^{\min} = 1.2 \text{ \AA}^{-1} \text{ and } k_i^{\max} = 2.6 \text{ \AA}^{-1}$$

Since  $k = 2\pi / \lambda$ ,  $k_i^{\min}$  corresponds to the maximum wavelength  $\lambda_i^{\max} = 5.2 \text{ \AA}$ , and  $k_i^{\max}$  to the minimum wavelength  $\lambda_i^{\min} = 2.4 \text{ \AA}$

### **E3**

(i) We have  $Q_{220} = 2\pi / d_{220} = \sqrt{8}(2\pi / a_0)$  so that  $Q_{220} = 3.20 \text{ \AA}$ .

Figure F1a shows the vectors  $\mathbf{k}_i$ ,  $\mathbf{k}_f$  and  $\mathbf{Q}$  for the 220 reflection.

(ii) Setting  $\mathbf{k}_i = \mathbf{k}_f$  in the scattering triangle equation;

$$Q^2 = k_i^2 + k_f^2 - 2k_i k_f \cos\phi$$

we get

$$\phi = 2 \sin^{-1} (Q/2k_i)$$

and so

$$\phi = 76^\circ$$

(iii) In the case of elastic scattering the scattering angle  $\phi$  is twice the Bragg angle  $\theta_B$

### **E4.**

See Figure E1a.

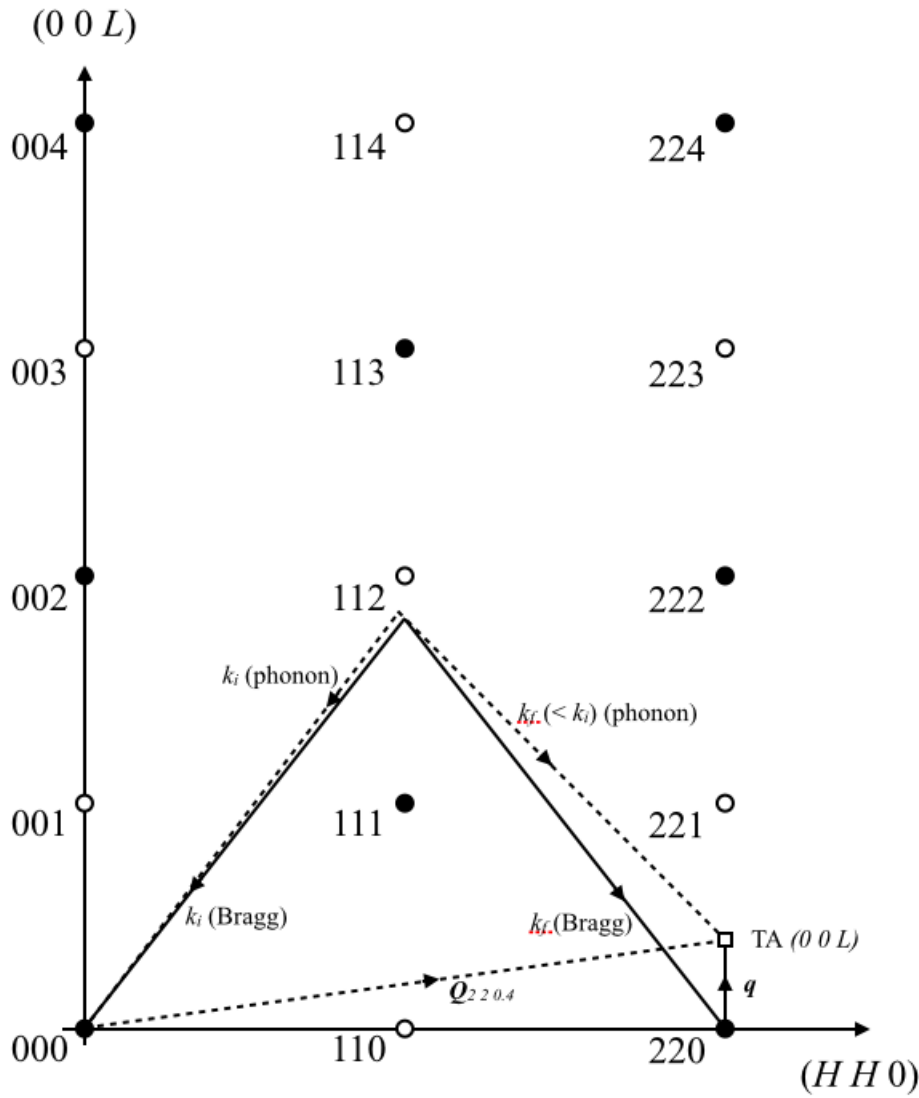


**Figure E1a.** Reciprocal lattice construction for 220 Bragg scattering and for inelastic scattering by the transverse acoustic [00L] phonon.

## E5.

The vector  $Q_{220.4}$  (Figure F1a) has a magnitude of

$$Q_{220.4} = (2\pi / a_0) \times \sqrt{(4 + 4 + 0.16)} = 3.228 \text{ \AA}^{-1}$$

We have  $E_i^{max} = 14$  meV and  $\Delta E = 3$  meV. Hence for neutron energy loss  $E_f = 11$  meV and for neutron energy gain  $E_f = 17$  meV. Using eqn. (E4) we get:

$k_f = 2.304 \text{ \AA}^{-1}$  for energy loss and  $k_f = 2.864 \text{ \AA}^{-1}$  for energy gain. From eqn. (E2) we then have:

$\phi = 82.1^\circ$  (energy loss) and  $\phi = 72.2^\circ$  (energy gain).

## E6.

The resolution is best for small  $k_f$ , i.e. for energy loss. In Figure E1a the vectors  $\mathbf{k}_i$  and  $\mathbf{k}_f$  are drawn for this configuration.

## E7.

(i) At 300K:  $n(E) = 8.1$  for energy gain and  $n(E) + 1 = 9.1$  for energy loss.

At 0K:  $n(E)=0$  for energy gain and  $n(E) + 1 = 1$  for energy loss.

(ii) Thus it doesn't make much difference at 300K whether one works in energy gain or in energy loss, but at low temperatures one must work in energy loss.

## E8.

No. Not with this value of the incident wavelength.

We have

$$Q_{440} = 2Q_{220} = 6.46 \text{ \AA}^{-1}$$

$k_i + k_f = 4.904 \text{ \AA}^{-1}$  in energy loss, and  $k_i + k_f = 5.464 \text{ \AA}^{-1}$  in energy gain. Hence  $k_i + k_f < Q$  and it is impossible to close the scattering triangle (Figure E2) in either case.

## E9.

Since potassium is cubic, the dispersion relationship shown in Fig. F9 for  $\mathbf{q} \parallel$  to (001) also applies to  $\mathbf{q} \parallel$  to (100). The LA mode (longitudinal acoustic) will have a higher frequency for a given  $\mathbf{q}$  than the TA (transverse acoustic) mode (due to Hooke's Law – transverse modes cause less longitudinal displacement than longitudinal modes).

$\mathbf{Q} = [2.5 \ 0 \ 0]$  is equivalent to  $\mathbf{Q} = [0 \ 0 \ 0.5]$ . Therefore, reading from the plot gives the phonon energy for the LA  $[0.5 \ 0 \ 0]$  as  $\sim 1.8$  THz, and for the TA  $[0.5 \ 0 \ 0]$  as  $\sim 1.6$  THz.

The final energy is fixed at  $E_f = 3.5$  THz, so for neutron energy loss

$$E_i = 3.5 + 1.8 = 5.3 \text{ THz} = 22.1 \text{ meV (LA)}$$

$$E_i = 3.5 + 1.6 = 5.1 \text{ THz} = 21.2 \text{ meV (TA)}$$

## F. High resolution spectroscopy (TOF, backscattering and Spin-Echo)

### **F1.**

(i)  $E = \frac{1}{2} * m * v^2$  and  $v = L/t$   
 $E = \frac{1}{2} * m * (L/t)^2$

Differentiating...  $\Delta E = \frac{1}{2} * m * L^2 * (-2) * t^{-3} * \Delta t$

Dividing ....  $\Delta E/E = [\frac{1}{2} * m * L^2 * (-2) * t^{-3} * \Delta t] / [\frac{1}{2} * m * L^2 * t^2]$   
 $\Delta E/E = 2\Delta t/t$

(ii) First we need to calculate the energy of the 6.27 Å neutron.

$$E (\text{meV}) = 81.81/\lambda^2 (\text{\AA}) = 2.08 \text{ meV}$$

Thus  $\Delta E/E = 1/2080 = 4.805 \times 10^{-4}$   
and  $\Delta t/t = \frac{1}{2} * \Delta E/E = 2.403 \times 10^{-4}$

(ii) The contribution to the resolution in the case of the moderator pulse uncertainty is then:

$$\Delta t/t = \Delta t_{\text{mod}}/t = 120 \mu\text{s}/t$$

Remembering that the velocity of a 6.68 Å was 594.3m/s and the distance to the sample was 36.41m, so that the time of arrival at the sample is  $t = 36.41/594.3 = 61265 \mu\text{s}$ . Then,

$$\Delta t/t = \Delta t_{\text{mod}}/t = 120 \mu\text{s}/61265 \mu\text{s} = 1.96 \times 10^{-3}$$

$$\Delta E/E = 2 \Delta t/t = 3.92 \times 10^{-3}$$

$$\Delta E = 3.92 \times 10^{-3} \times 1.843 \text{ meV} = 7.2 \mu\text{eV}$$

**In its present state, IRIS could never reach a resolution of 1 μeV**  
because the primary contribution is already 7μeV.

Ways to improve the resolution include:

(a) Make the length of the instrument much longer

For  $\Delta E/E = 1/1843 = 5.426 \times 10^{-4} = 2 \times 120 \mu\text{s}/t$

Thus  $t = 442,315 \mu\text{s}$ , and so  **$L \approx 263 \text{ m}!!$**

- (b) Reduce the moderator pulse width by adding a so-called pulse shaping chopper. If we stick to the IRIS length of 36.41m, we would need a pulse width of:

For  $\Delta E/E = 1/1843 = 5.426 \times 10^{-4} = 2 \times \Delta t_{\text{mod}}/61265 \mu\text{s}$

Thus  $\Delta t_{\text{mod}} = 16.6 \mu\text{s}$

- (iv) First calculate the velocity of a  $6.27\text{\AA}$  neutron. We know that the energy is 2.08 meV, thus:

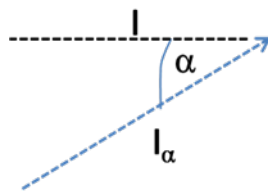
$$E = 2.08 \times 1.6 \times 10^{-22} (\text{J}/\text{meV}) = \frac{1}{2} * 1.675 \times 10^{-27} * v^2$$

and so  $v = 630.4 \text{ m/s}$

The arrival time is then  $t = 100/630.4 = 0.159 \text{ s}$

So, for  $\Delta E/E = 4.805 \times 10^{-4}$ ,  $\Delta t/t = 2.4 \times 10^{-4}$ ,  $\Delta t = 38.2 \mu\text{s}$

- (v) We need to calculate the flight path difference which will be:



$$(l_a - l) * N$$

where  $N$  is the number of reflections along the flight path.

First find an expression for  $(l_a - l)$ . Look at the right angled triangle formed.

$$\cos \alpha = l/l_a, \quad (l_a - l) = (l/\cos \alpha) - l = l * [(1/\cos \alpha) - 1]$$

$$\text{Thus } \Delta L = (l_a - l) * N = N * l * [(1/\cos \alpha) - 1]$$

$$\text{Thus } \Delta L/L = N * l * [(1/\cos \alpha) - 1] / N * l = [(1/\cos \alpha) - 1]$$

Since  $L = v * t$ ,  $\Delta L/L = \Delta t/t$  at constant velocity.

In our case,  $\alpha = 0.1^\circ * 2 * 6.27 = 1.254^\circ$

So  $\Delta L/L = 2.396 \times 10^{-4} = \Delta t/t$  and thus  $\Delta L = 2.4 \text{ cm}$ .

- (vi) To keep the 1eV resolution we can allow a time uncertainty of  $\Delta t_{\text{CH}_2} = 38.2 \mu\text{s}$  for a  $6.27\text{\AA}$  neutron just like we calculated in part (iv) because  $\text{CH}_2$  is positioned at  $L = 100\text{m}$ .

Mechanically, the chopper opening time is defined as  $\Delta t_{\text{CH}_2} = (\beta/360)/f$ , where  $\beta$  is the chopper window angular opening and  $(\beta/360)$  is called the duty cycle which equals the fraction of neutrons

transmitted by the chopper. A typical value of the duty cycle is 0.01. Calculate the chopper frequency needed to achieve the chopper opening time calculated before.

$$f = (\beta/360)/\Delta t_{CH2} = 0.01/38.2 \times 10^{-6} = 261.8 \text{ s}^{-1}$$

$$f \approx 262 \text{ Hz} = 15720 \text{ rpm}$$

(1Hz = 60 rpm)

## F2.

(vii) Starting from the relationship between energy and wavelength:

$$E = 81.81/\lambda^2$$

$$\text{Differentiating gives ...} \quad \Delta E = -2 * 81.81 * \Delta \lambda / \lambda^3$$

$$\text{Dividing gives ...} \quad \Delta E/E = 2 \Delta \lambda / \lambda$$

(viii) Starting from Bragg's Law:

$$\text{Bragg's Law says that} \quad \lambda = 2d \sin \theta$$

$$\text{Differentiating gives} \quad \Delta \lambda = 2 \Delta d \sin \theta + 2d \cos \theta \cdot \Delta \theta$$

$$\text{Dividing gives} \quad \Delta \lambda / \lambda = \Delta d / d + \cot \theta \cdot \Delta \theta$$

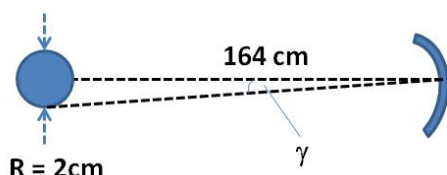
The idea is to minimise the contributions to the energy resolution so at the backscattering condition of  $\theta=90^\circ$ , the  $\cot \theta \cdot \Delta \theta$  term disappears.

$$(a) \quad \Delta E/E = 2 \Delta \lambda / \lambda = 2 (\Delta d / d + \Delta \theta^2 / 8)$$

$$\text{For Si(111): } \Delta E/E = 2 \Delta \lambda / \lambda = 2 (1.86 \times 10^{-5}) = 3.72 \times 10^{-5}$$

$$\text{For PG(002): } \Delta E/E = 2 \Delta \lambda / \lambda = 2 (2 \times 10^{-3}) = 4 \times 10^{-3}$$

(b)



$$\gamma = \tan^{-1} (2/164) = 0.7^\circ = 0.7 \times \pi/180 = 0.0122 \text{ rad}$$

$$\Delta \lambda / \lambda \sim (0.0122)^2 / 8 = 1.86 \times 10^{-5}$$

### F3.

(ix)  $t_{\text{NSE}} = \hbar\gamma BL/(m_n v_n^3)$   
 $t_{\text{NSE}} = (1.06 \times 10^{-34} * 1.832 \times 10^8 * 0.25)/1.675 \times 10^{-27} * (630.4)^3$   
 **$t_{\text{NSE}} = 11.6 \text{ ns}$**

(x)  $E_{\text{NSE}} = h/t_{\text{NSE}} = 4.136/11.6 = 0.36 \text{ eV}$

(xi) Lower flux at longer wavelengths and the Q-range will change since  
 $Q=4\pi\sin\theta/\lambda$ .

## G. Small Angle Scattering

### **G1.**

$$(a) R_G = \sqrt{-3 \times \text{gradient}}$$

Therefore, if the gradient given in Figure G2 is taken:

$$R_G = \sqrt{-3 \times -172.62}$$

$$R_G = \underline{\underline{22.75 \text{ \AA}}}$$

b) To check for concentration based inter-particle effects and aggregation.

### **G2.**

a)

(i) Formula for monomers is  $C_{13}H_{14}O_4$

$$\text{so MW} = 13 \times 12.011 + 14 \times 1.008 + 4 \times 15.999 = 234.25 \text{ g mol}^{-1}$$

$$Nb = \frac{N_A \cdot \rho}{MW} \sum_i b_i$$

$$= N \sum_i b_i$$

$$(N_A \text{ mol}^{-1} \times 1.27 \text{ g cm}^{-3} / 234.25 \text{ g mol}^{-1}) \times b(13C + 14H + 4O)$$

$$= (6.022 \times 10^{23} \text{ mol}^{-1} \times 1.27 \text{ g cm}^{-3} / 234.25 \text{ g mol}^{-1}) \times (13 \times 6.65 + 14 \times (-3.742) + 4 \times 5.803) \times 10^{-13} \text{ cm}$$

$$= 3.265 \times 10^{21} \times 5.727 \times 10^{-12} \text{ cm}$$

$$= \underline{\underline{1.87 \times 10^{10} \text{ cm}^{-2}}}$$

(ii) In  $D_2O$  because the difference between the SLD of  $H_2O$  and the polymer is much smaller than the difference between the SLD of  $D_2O$  and the polymer. ALSO H has a high incoherent cross-section so results in a large amount of incoherent scattering from the H in the solvent, increasing the background in that system. Ideally use as little H as possible in SANS samples.

b) Formula for deuterated tetradecane:  $C_{14}D_{30}$

$$\text{so MW} = 14 \times 12.011 + 30 \times 3.008 = 228.39 \text{ g mol}^{-1}$$

$$Nb = \frac{N_A \cdot \rho}{MW} \sum_i b_i$$

$$= N \sum_i b_i$$

$$(N_A \text{ mol}^{-1} \times 0.765 \text{ g cm}^{-3} / 228.39 \text{ g mol}^{-1}) \times b(14C + 30D)$$

$$= (6.022 \times 10^{23} \text{ mol}^{-1} \times 0.765 \text{ g cm}^{-3} / 228.39 \text{ g mol}^{-1})$$

$$\times (14 \times 6.65 + 30 \times 6.674) \times 10^{-13} \text{ cm}$$

$$= \underline{\underline{5.92 \times 10^{10} \text{ cm}^{-2}}}$$

c) (i) the polymer rim around the phospholipids

$$(\text{ii}) \text{ core sld} = 0.78 \times 6.34 \times 10^{10} \text{ cm}^{-2} + 0.22x(-0.562 \times 10^{10} \text{ cm}^{-2}) = 4.87 \times 10^{10} \text{ cm}^{-2}$$

this is lower than calculated for tetradecane above. Thus there must be hydrogenous material in the core, which is probably the styrene groups from the polymer belt.

d)

(i) The Guinier region for very large spheres would be outside the Q-range of SANS, so we would see slope of -2 on log I vs log Q graph, changing to -4 at very high Q due to smooth surface structure, limiting Porod scattering. Fringes would appear in the data due to the thickness of the lamellae (membrane). See figure G2a below.

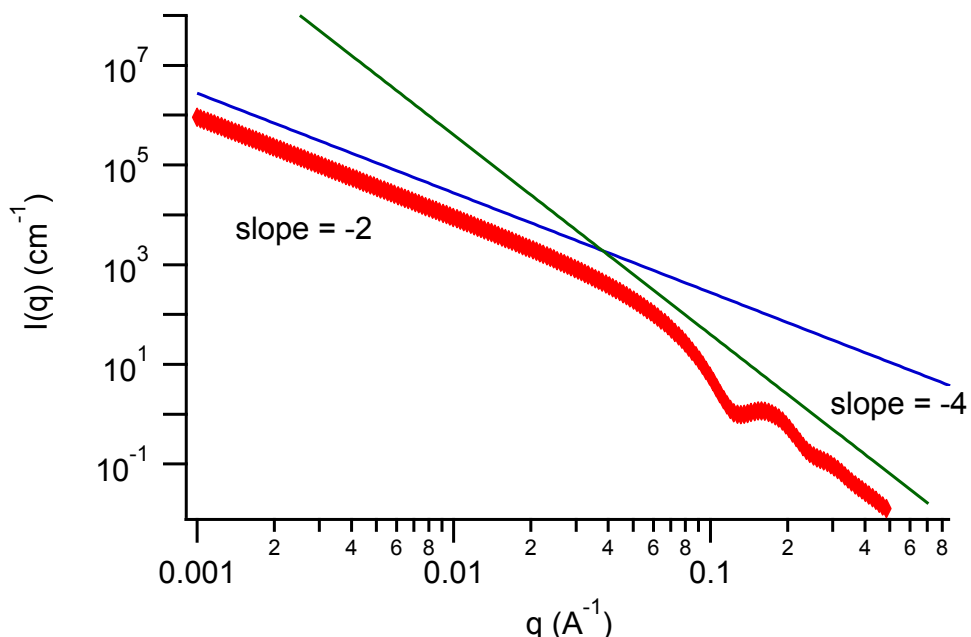


**Figure G2a** Guinier plot ( $\log(I)$  vs.  $\log(Q)$ ) of large spheres in solution

(ii) stacked discs would give scattering due to the distance between the discs which would cause peaks similar to those from a lamellar phase. The scattering would be anisotropic in the horizontal direction due to the vertical alignment of the stacked discs (see figure 3).

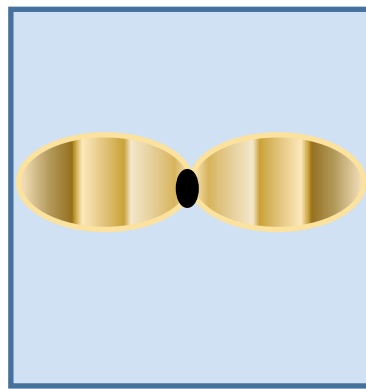


**Figure J3a** SANS pattern expected from oriented stacked nanodiscs

(iii) We would need to use multiple contrasts to obtain detailed structural information, so we should suggest doing experiments with deuterated polymer, lipid, protein & solvent to obtain as many different scattering patterns as possible. See Figure J4a below

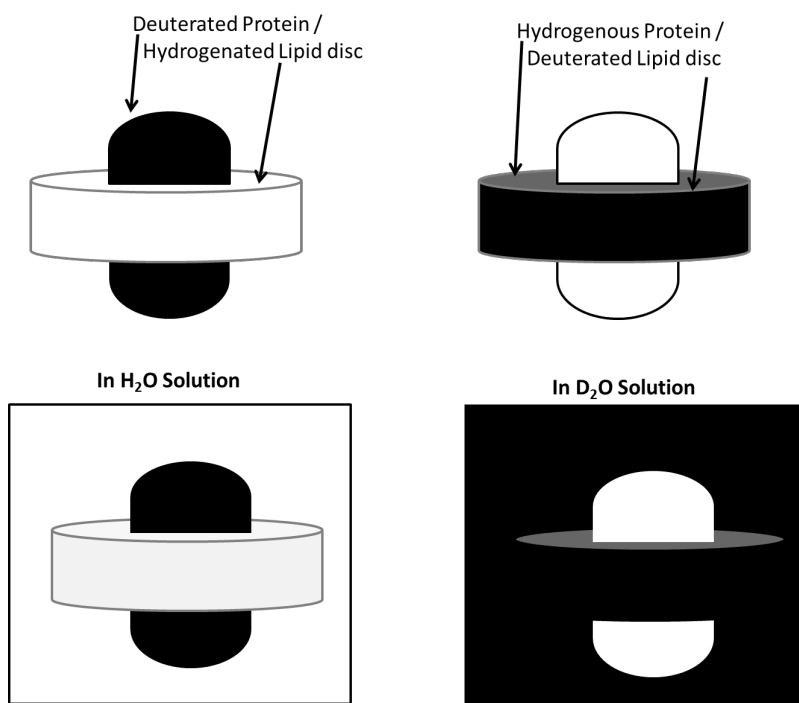


**Figure J4a** Illustration of contrast matching in the protein / nanodisc system

Once a suitable contrast has been chosen, in which the contribution to the SANS of the nanodisc has been removed by contrast matching the disc to the solvent, the analysis of the scattering from the protein can be examined. If a crystal structure for the protein has been deposited in the protein

databank the scattering from the high resolution structure can be modelled and compared to the experimental data using packages such as Cryson and Crysol in the ATSAS package.

A popular approach to analysing the shape of proteins from SANS/SAXS is dummy atom modelling by simulated annealing, which allows for the low resolution structure of the particulate from the scattering data. In this approach, heuristic monte carlo like algorithms are employed to perform a “trial and error” modelling using beads within a user defined volume. In this approach an automated shape search within a volume which encloses the protein maximum dimensions is performed. The space is filled with densely packed spheres which can either belong to the protein or the solution. Starting with a random distribution of solution and protein “beads” within the search volume the model is randomly modified to find a shape which fits the experimental data. As proteins often have complex shapes which cannot be defined by simple shape models such as spheres, ellipsoids etc this method is popular with the biological small angle scattering community and is performed using software such as Dammin, Gasbor and MONSA (for multi-contrast data sets).

e) slope =  $\frac{-R_t^2}{12}$ ,

so here the slope,  $-121 \text{ \AA}^2 = \frac{-R_t^2}{12}$ , so  $R_t = \underline{\underline{38.1 \text{ \AA}}}$ ,

Assumption is that the particle is in a dilute solution (no inter-particle interactions)

## H. Reflectometry

### HI.

a) Given  $SLD = Nb = N \sum_i b_i$  (Need to watch your units!!!!)

Where  $N$ = number density of atoms in atoms per  $\text{\AA}^3$ ,  $b$ = scattering length in units of fm ( $\times 10^{-15}$  m) and :

$$Nb = \frac{N_A \cdot \rho}{M_w} \sum_i b_i = N \sum_i b_i$$

Note:  $1 \times 10^{-24} \text{ cm}^3$  in  $1 \text{\AA}^3$ , 1 fm is  $1 \times 10^{-5} \text{\AA}$

- Convert units first, as this is much easier if everything is consistently in grams,  $\text{\AA}$  and moles.

$$\begin{aligned} \text{Density of } SiO_2 & \text{ is } 2533 \text{ kgm}^{-3} = \underline{\underline{2.533 \times 10^{-24} \text{ g\AA}^{-3}}} \\ b(Si) &= 4.1491 \text{ fm} = \underline{\underline{4.1491 \times 10^{-5} \text{\AA}}} \\ b(O) &= 5.803 \text{ fm} = \underline{\underline{5.803 \times 10^{-5} \text{\AA}}} \\ \text{Molar mass Si} &= \underline{\underline{28.0855 \text{ g mol}^{-1}}} \\ \text{Molar mass O} &= \underline{\underline{15.999 \text{ g mol}^{-1}}} \end{aligned}$$

- Then Calculate  $\sum_i b_i$

$$b(SiO_2) = b(Si) + 2*b(O) = 4.1491 + 2*5.803 = \underline{\underline{15.7551 \times 10^{-5} \text{\AA}}}$$

- Then calculate the molecular weight of  $SiO_2$

$$M_w(SiO_2) = 28.0855 + 2*(15.999) = \underline{\underline{60.0835 \text{ g mol}^{-1}}}$$

- Calculate the Number density  $N = \frac{N_A \cdot \rho}{M_w}$   
 $N_{SiO_2} = 6.022 \times 10^{23} \times 2.533 \times 10^{-24} / 60.0835 = \underline{\underline{0.02539 \text{ atoms \AA}^{-3}}}$

- Calculate  $N \sum_i b_i$

$$SLD = 0.02539 \times 15.7551 \times 10^{-5} = \underline{\underline{4.00 \times 10^{-6} \text{\AA}^{-2}}}$$

b) Repeat solution for a)

- Convert units first, as this is much easier if everything is consistently in grams, Å and moles.

$$\begin{aligned} \text{Density of Ni is } 8908 \text{ kgm}^{-3} &= \underline{\mathbf{8.908 \times 10^{-24} \text{ kg}\text{\AA}^{-3}}} \\ b (\text{Si}) = 10.3 \text{ fm} &= \underline{\mathbf{10.3 \times 10^{-5} \text{ \AA}}} \\ \text{Molar mass Ni} &= \underline{\mathbf{58.6934 \text{ g mol}^{-1}}} \end{aligned}$$

- Calculate the Number density  $N = \frac{N_A \cdot \rho}{M_w}$   
 $N_{\text{Ni}} = 6.022 \times 10^{23} \times 8.908 \times 10^{-24} / 58.6934 = \underline{\mathbf{0.0914 \text{ atoms \AA}^{-3}}}$
- Calculate  $N \sum_i b_i$

$$\text{SLD} = 0.091397 \times 10.3 \times 10^{-5} = \underline{\mathbf{9.414 \times 10^{-6} \text{ \AA}^{-2}}}$$

c) Magnetic Scattering Length Density ( $\text{SLD}_m$ ) is given by:

$$SLD_m = \sum_i^J N_i \mathbf{p}_i = C \sum_i^J N_i \mu_i = C' \mathbf{m} = -\frac{m_n}{2\pi\hbar^2} \mu_n \sum_i^J \mathbf{M}_i$$

- Where for magnetic moment per formula units,  $\mu$ , expressed in units of Bohr Magnetons  $\mu_B$ , then  $C = 2.645 \times 10^{-5} \text{ \AA} \mu_B^{-1}$
- Or if the Volume magnetisation density,  $\mathbf{m}$ , is known in units of Tesla, then  $C = 2.911 \times 10^{-5} / 4\pi \text{ \AA}^{-2} \text{ T}^{-1}$
- Or if  $\mathbf{m}$  is in units of emu/cm<sup>3</sup> then  $C = 2.853 \times 10^9 \text{ \AA}^{-2} \text{ cm}^3 / \text{emu}$

$N_i$  = number density of magnetic atoms in units of atoms Å<sup>-3</sup>

$\mathbf{p}_i$  = Magnetic scattering length in units of fm

$\mu_n$  = magnetic moment of the neutron

$\mathbf{M}_i$  = Magnetisation (emu)

- $\text{SLD}_m = \pm CN \mu_i = \pm 2.645 \times 10^{-5} \times 0.091397 \times 1.8 = \underline{\mathbf{\pm 4.351 \times 10^{-6} \text{ \AA}^{-2}}}$

d)

- $SLD_{Ni\pm} = SLD_{Ni(\text{structure})} + SLD_{Ni(\text{Magnetic})}$

$$SLD_{Ni+} = (9.4139 + 4.3514) \times 10^{-6} \text{ \AA}^{-2} = \underline{\underline{13.765 \times 10^{-6} \text{ \AA}^{-2}}}$$

$$SLD_{Ni-} = (9.4139 - 4.3514) \times 10^{-6} \text{ \AA}^{-2} = \underline{\underline{5.063 \times 10^{-6} \text{ \AA}^{-2}}}$$

## H2.

a) Because it makes the simulation angle and wavelength dependent and therefore comparable to other neutron reflectivity data from other neutron sources.

b) Construct the basic scattering diagram:

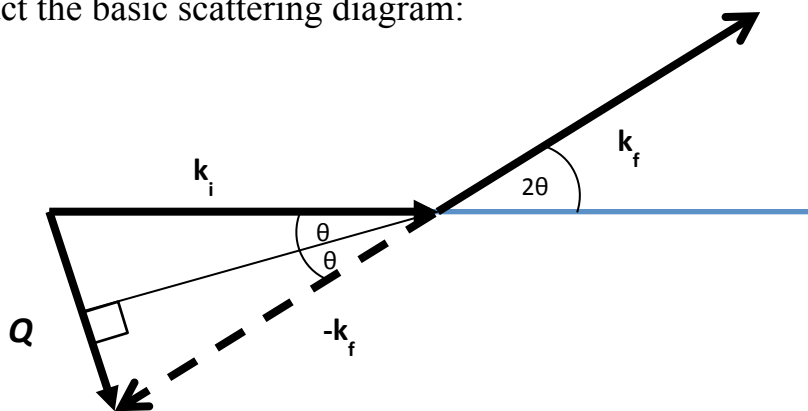


**Figure H1a, basic scattering diagram**

- For elastic scattering then  $|k_i| = |k_f| = \frac{2\pi}{\lambda}$  (A)
- From QM momentum transfer is expressed as  $Q = k_i - k_f$
- Take the vertical components, defined in scattering as z direction

$$Q_z = k_i \sin \theta - k_f \sin \theta$$

$$Q_z = k_i \sin \theta + k_f \sin \theta$$

- Recalling A then this can be rewritten as:

$$Q_z = \frac{4\pi}{\lambda} \sin \theta$$

### H3

a) Start with the Snells law :

$$n = \frac{n_1}{n_0} = \frac{\cos \theta_i}{\cos \theta_t}$$

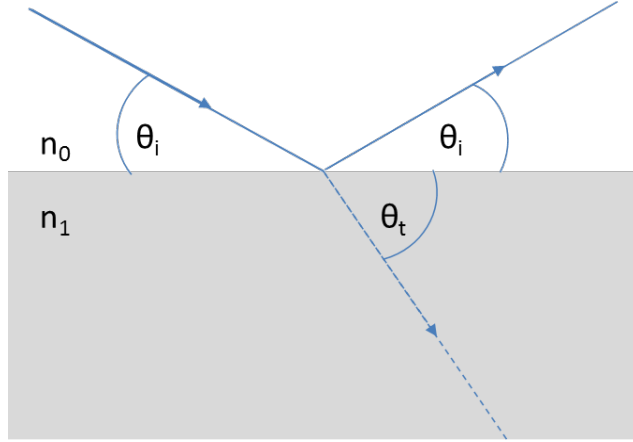


**Figure H2a, Snell's law of reflection**

- At total reflection  $\theta_i = \theta_c$  and  $\theta_t = 0$  therefore  $\cos \theta_t = \cos 0 = 1.0$
  - Therefore:
  -
- $$n = \frac{n_1}{n_0} = \cos \theta_c \quad (\text{A})$$

Recall basic trig identity:  $\sin^2 \theta + \cos^2 \theta = 1$

Then taking the square of (A) allows the following via the trig identity:

$$\begin{aligned} n &= \cos \theta_c \\ n^2 &= \cos^2 \theta_c \quad (\text{Then by the trig identity}) \\ n^2 &= 1 - \sin^2 \theta_c \quad (\text{Rearrange to get}) \\ \sin^2 \theta_c &= 1 - n^2 \\ \sin \theta_c &= \sqrt{1 - n^2} \end{aligned} \quad (\text{D})$$

$$\text{Recall } Q_z = \frac{4\pi}{\lambda} \sin \theta \quad \text{giving} \quad Q_c = \frac{4\pi}{\lambda} \sin \theta_c \quad (\text{E})$$

Then substitute (\*) into (D) to get:

$$\sin \theta_c = \sqrt{1 - 1 + \frac{\lambda^2 N b}{\pi}}$$

$$\sin \theta_c = \sqrt{\frac{\lambda^2 Nb}{\pi}}$$

Then substitute in (E) to get:

$$\frac{Q_c \lambda}{4\pi} = \sqrt{\frac{\lambda^2 Nb}{\pi}}$$

Rearrange to get

$$Q_c = \sqrt{16\pi Nb}$$

b) Ni/air interface so can use calculated values for Ni+/- from question 1

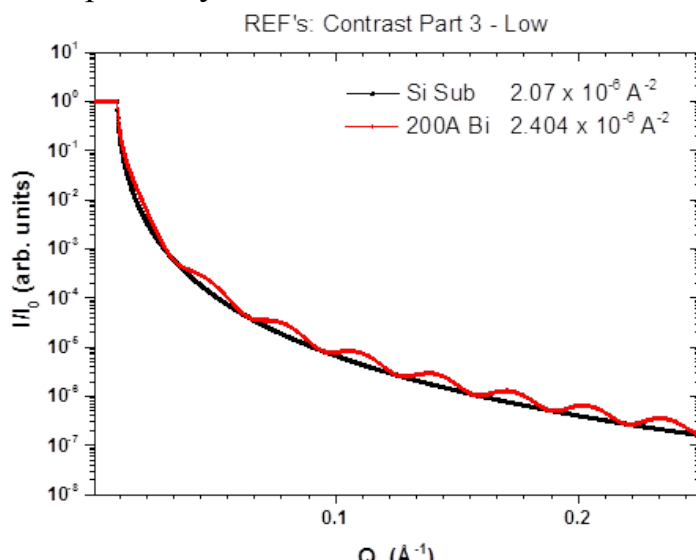
$$Q_c (\text{Ni}^+) = \sqrt{16\pi \times (13.765 \times 10^{-6})} = \underline{0.0263 \text{ \AA}^{-1}}$$

$$Q_c (\text{Ni}^-) = \sqrt{16\pi \times (5.063 \times 10^{-6})} = \underline{0.0160 \text{ \AA}^{-1}}$$

c) The difference in Q between the two critical edge positions is a direct measure of the total magnetic moment in the thin film. The taking this difference subtracts the structural parts hence all that is left is the magnetic component.

#### H4a

Bi and Si have very similar contrasts so look very similar in reflectivity. If the Bi or Si have even slightly rough surfaces or interfaces then it will not be distinguishable from each other and the reference layer will look like the Si substrate and not appear to be there. The figure shows the perfectly flat case for 200A of Bi on a perfectly flat Si substrate.



H3a, Bi layer on Si

## H5a

- a) the thickness of the Kessig fringes can be related back to Braggs law via the small angle approximation:

$$n\lambda = 2d \sin \theta$$

$$d = \frac{\lambda}{2\Delta\theta}$$

Which by substituting the relation for:

$$Q_z = \frac{4\pi}{\lambda} \sin \theta$$

This becomes:

$$d = \frac{2\pi}{\Delta Q}$$

$$\Delta Q1 = \frac{2\pi}{0.00625} = \mathbf{1005.3 \text{ \AA}}$$

$$\Delta Q2 = \frac{2\pi}{0.00731} = \mathbf{589.5 \text{ \AA}}$$

$$\Delta Q3 = \frac{2\pi}{0.00819} = \mathbf{767.2 \text{ \AA}}$$

$$\Delta Q4 = \frac{2\pi}{0.00814} = \mathbf{771.9 \text{ \AA}}$$

- b) Because we have neglected the n component in Braggs Law.

- c) You should work inside of the Born approximation and take the difference of two fringes as far from the critical edge as you can. Hence the best estimate is the last one  $\mathbf{772 \text{ \AA}}$ .

## I: Polarized Neutrons

**I1.** a) Flipping ratio:  $F = N_+ / N_- = 51402 / 1903 = 27 \pm 0.6$

$$\{\text{error bar } dF = \sqrt{\left(\frac{dN_+}{N_-}\right)^2 + \left(\frac{dN_- N_+}{N_-^2}\right)^2} \Rightarrow dF = 0.63\}$$

Therefore, the polarization is:  $P = F - 1 / F + 1 = 0.929 \pm 0.002$

$$\{\text{error bar } dP = \left(\frac{2}{(F+1)^2}\right)dF \Rightarrow dF = 0.002\}$$

b) Systematic errors in this measurement will largely arise from background contributions from the instrumental environment. In order to measure a reliable flipping ratio, the  $N_+$  and  $N_-$  counts must be measured with and without the sample in the beam. The flipping ratio is then given by

$$F = \frac{N_+^{\text{sample}} - N_+^{\text{empty}}}{N_-^{\text{sample}} - N_-^{\text{empty}}}$$

Other sources of systematic error will be different values of the polarizing power of the polarizer and analyser, in addition to the finite flipping efficiency of the flipper.

**I2.** a) The adiabacity parameter is given by  $E = \frac{\omega_L}{\omega_B}$

The Larmor frequency,  $\omega_L = \gamma B$ , where the gyromagnetic ratio,  $\gamma$ , is given by the ratio of the neutron magnetic moment to its angular momentum ( $= \frac{1}{2}\hbar$ ). Therefore:  $\omega_L = 2\mu_B B / \hbar = 1.83 \times 10^8 B \text{ rad s}^{-1}$  with  $B$  given in T. In this example,  $B = 3 \text{ mT}$  and is constant in magnitude, therefore

$$\omega_L = 5.49 \times 10^5 \text{ rad s}^{-1}$$

The rotation frequency of the guide field in the neutron rest frame is

$$\omega_B = \frac{d\theta}{dx} \times v = \frac{\frac{\pi}{2}}{0.1} \times v = 15.71v$$

Expressing  $v$  in terms of  $\lambda$ :

$$E = \frac{h^2}{2m_n\lambda^2} = \frac{m_n v^2}{2} \Rightarrow v = \frac{h}{m_n \lambda} = \frac{3956}{\lambda} \text{ with } v \text{ in ms}^{-1} \text{ and } \lambda \text{ in \AA}.$$

Therefore:

$$\omega_B = 3.11 \times 10^4 \text{ rad s}^{-1}$$

The adiabacity parameter is therefore: **E = 17.7** and the field/flipper design should successfully propagate the neutron polarization and flip the spins without significant depolarization.

b) The design could be improved by either increasing the guide fields (and the current in the Dabbs foil) or by lengthening the distance over which the field rotates by 90°.

**I3.** a) The expression for the differential cross-section of a polarized neutron beam of polarization ( $\mathbf{P}$ ) from a ferromagnetic crystal magnetised along the direction ( $\mathbf{\eta}$ ) reflecting from the *HKL* Bragg plane, is of the form

$$\frac{d\sigma}{d\Omega} = F_N^2 + F_M^2 + 2F_N F_M [\mathbf{P} \cdot \hat{\mathbf{\eta}}]$$

If we consider an initially unpolarized beam as a superposition of equal populations of “spin-up” and “spin-down” neutrons, then the number of neutrons scattered in each spin-state will be proportional to the two cross sections.

$$\begin{aligned} n_+ &\propto \left. \frac{d\sigma}{d\Omega} \right|_{\mathbf{P} \parallel \mathbf{\eta}} = (F_N + F_M)^2 \\ n_- &\propto \left. \frac{d\sigma}{d\Omega} \right|_{\mathbf{P} \nparallel \mathbf{\eta}} = (F_N - F_M)^2 \end{aligned}$$

Therefore, the polarization is:

$$P = \frac{n_+ - n_-}{n_+ + n_-} = \frac{(F_N + F_M)^2 - (F_N - F_M)^2}{(F_N + F_M)^2 + (F_N - F_M)^2} = \frac{2F_N F_M}{F_N^2 + F_M^2}$$

Note that the sign of the polarization depends on the signs of the unsquared magnetic and nuclear structure factors. In the case of Heusler alloy, these signs are opposite, and the polarization is oriented opposite to the magnetisation (i.e. spin-down)

b) Making the substitution,  $x = F_N/F_M$ , we have

$$P = \frac{2x}{x^2+1}$$

Differentiating with respect to  $x$

$$\frac{dP}{dx} = \frac{2-2x^2}{(x^2+1)^2}$$

The maximum polarization is therefore found for  $x = \pm 1$ . *i.e.* When the nuclear and magnetic structure factors are equal.

**I4.** The first rule of thumb in magnetic polarized neutron scattering is that spin-flipped neutrons will only be produced by components of the sample magnetisation perpendicular to the neutron polarization direction. [This is an extremely useful rule to bear in mind during all polarized neutron experiments.] Therefore, if we are scattering neutrons from a fully magnetised scatterer (*i.e.* a ferromagnet for example) – magnetised in the direction of the neutron polarization (which is an experiment necessity), then there will be no perpendicular components of the magnetisation, and therefore no spin-flip scattering. We can therefore dispense with the analysers, since the scattered beam remains fully polarized

## J. Spin-Echo Small-Angle Neutron Scattering

### **J1**

1.  $\varphi = \frac{\gamma_n m \lambda dB}{h} = 3323$  radian, corresponding to 528 rotations

[ $1.832e8 * 1.67e-27 * 2e-10 * 0.18 * 0.2 / 6.63e-34$ ].

This indicates that the uniformity of the line integrals should be at least an order of magnitude better than 1/528 to maintain the polarisation.

2. The length of the path through the foil with a thickness  $t$  will be

$$l = \frac{t}{\sin(\vartheta_0)} . \text{ The precession in the foil will thus be } \varphi = \frac{\gamma_n m \lambda t B_s}{h \sin(\vartheta_0)} \text{ should be } \pi,$$

from which follows  $t = \frac{\varphi h \sin(\vartheta_0)}{\gamma_n m \lambda B_s} = 3.3 \mu\text{m}$

[ $3.14 * 6.63e-34 * \sin(3.14 * 5.5 / 180) / 1.832e8 / 1.67e-27 / 2e-10 / 1$ ].

This is indeed the thickness of the foils we use in Delft.

3. The precession due to a height difference with the optical axis of  $\delta y$

can be calculated from the geometry to be  $\varphi = \frac{2\gamma_n m \lambda B \delta y \cot(\vartheta_0)}{h}$ , in which

the factor of 2 is due to the precession before and after the  $\pi$ -flip. From this follows that sensitivity to an extra precession of  $\varphi = 2\pi/10$ , gives a height

sensitivity of  $\delta y = \frac{\varphi h}{2\gamma_n m \lambda B \cot(\vartheta_0)} = 1.64 \mu\text{m}$

[ $(2 * 3.14 / 10) * 6.63e-34 * \tan(\pi * 5.5 / 180) / 2 / 1.832e8 / 1.67e-27 / 2e-10 / 0.2$ ].

This is orders of magnitude smaller than one would achieve by using slits.

4. For a perfectly horizontal beam the precession in the two magnetic foil flippers will spin-echo. An angle  $\delta\theta$  with the optical axis over the length  $L$  between them will give rise to a height difference of  $\delta y = \delta\theta L$ .

Using the results of the previous calculation we get directly a sensitivity

over an angle of  $\delta\theta = \frac{\varphi h}{2\gamma_n m \lambda B L \cot(\vartheta_0)} = 1.26 \mu\text{rad}$

[ $(2 * 3.14 / 10) * 6.63e-34 * \tan(\pi * 5.5 / 180) / 2 / 1.832e8 / 1.67e-27 / 2e-10 / 0.2 / 1.3$ ].

This is impossible with conventional SANS.

5. For a straight non-scattered beam the precession in the two arms with reversed fields will spin-echo. We can now insert the wave vector

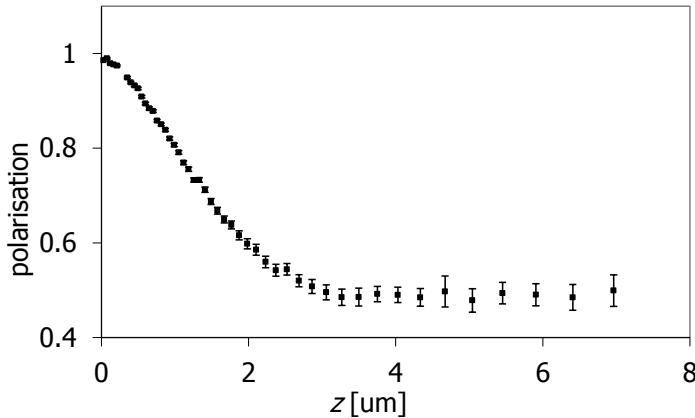
$Q = 2\pi\theta / \lambda$ , in the precession calculation

$$\varphi = \frac{2\gamma_n m \lambda B L \theta \cot(\vartheta_0)}{h} = \frac{\gamma_n m \lambda^2 B L \cot(\vartheta_0)}{h \pi} Q . \text{ From the definition } \varphi = \delta Q \text{ follows}$$

directly:  $\delta = \frac{\gamma_n m \lambda^2 L B \cot \theta_0}{\pi h}$  [M.Th. Rekveldt *et al.* Neutron Spin Echo, Lecture Notes in Physics 601 87-99 (2003)]

## J2

1.

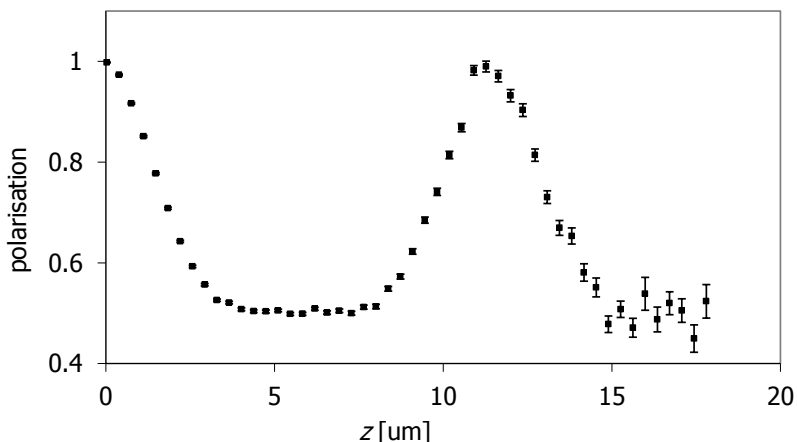


From the graph we see directly that the polarisation levels off at a spin-echo length of  $\delta = 4 \mu\text{m}$ , which corresponds to the maximum size present in the structure which is thus the diameter of  $2R$ , from which follows that

$R = 2 \mu\text{m}$ . The polarisation reaches a value of 0.5, from which we can calculate the scattering power  $\Sigma_t = -\ln(0.5) = 0.7$ . From the equation for the scattering power we derive that the volume fraction (for small values) has the value  $\phi = \frac{\Sigma_t}{\lambda^2 t (\Delta\rho)^2 \frac{3}{2} R} = 0.06$  [ $0.7/(2.1\text{e-}10)^2/0.005/(1.3\text{e}14)^2/1.5/2\text{e-}6$ ],

which indeed is small. [C. Rehm *et al.* J. of Appl. Cryst. 64 354-364 (2013)]

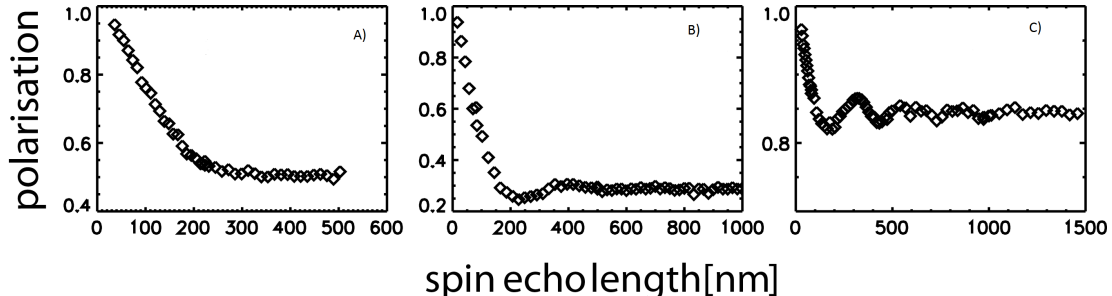
2.



The peak at the spin-echo length of  $12 \mu\text{m}$  corresponds to the period of the grating. The first peak levels off at  $4 \mu\text{m}$  corresponding to the trench width. This gives a volume fraction of  $\phi = 4/12 = 0.33$ . The  $\xi$  is equal to the thickness of the sample  $t$ , which is the depth of the trenches. Just as in the

previous exercise the polarisation levels of at a value of 0.5. From the equation of the scattering power we calculate  $t = \sqrt{\frac{\Sigma_t}{\lambda^2(\Delta\rho)^2\phi(1-\phi)}} = 40\mu\text{m}$  [ $\text{sqrt}(0.7/(2.1\text{e}-10)^2/(2.07\text{e}14)^2/0.33/0.67)$ ], which is indeed the depth. [M. Trinker *et al.* Nuclear Instruments and Methods in Physics Research A 579 1081–1089 (2007)]

3.



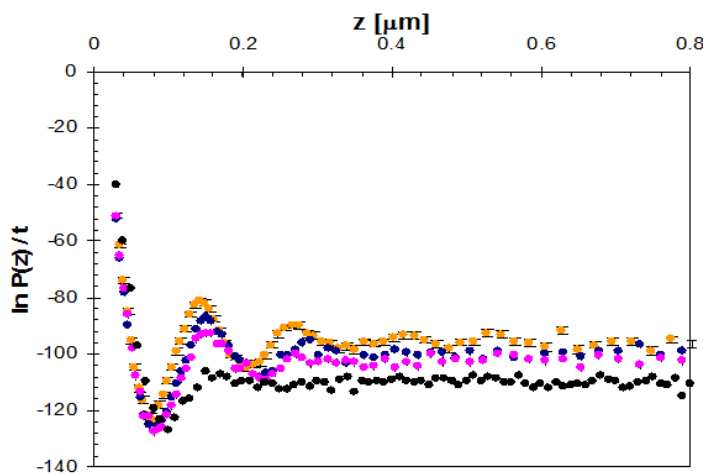
A) has the shape of the correlation function of a single sphere with diameter of 300 nm. No features are observed at higher spin-echo length, thus it corresponds to a low volume fraction: 0.055 volume fraction with a thickness of 10 mm.

B) shows one neighbour peak at a value just above the determined diameter, so it should correspond to a liquid phase. It is thus: 0.23 volume fraction with a thickness of 2 mm.

C) displays several neighbour peaks. It looks like a solid crystal, thus it has to be: 0.56 volume fraction in a cell with a thickness of 1 mm.

[T.Krouglov *et al.* J. Appl. Cryst. 36, 1417-1423 (2003)]

4.



Charged latex particles will repel each other, giving rise to a crystalline structure with many neighbour peaks as one observes for the yellow symbols. Adding salt will screen the Coulomb interaction as one sees for the brown symbols. The interaction potential can be fully determined from the measurements [K. van Gruijthuijsen *et al.*, EPL 106 28002 (2014)].

## K. Magnetic Elastic Scattering

### K1.

In order to answer this question, we use the convolution theorem which states that the Fourier transform of the convolution of two functions, is equal to the product of their Fourier transforms.

$$f(x) = g(x) \otimes h(x) \iff F(q) = G(q) \times H(q)$$

The equation for a Gaussian is:

$$g(x) = \frac{1}{\sqrt{2\pi\sigma^2}} \exp\left(-\frac{x^2}{2\sigma^2}\right)$$

The Fourier transform of this Gaussian is:

$$\begin{aligned} G(q) &= \frac{1}{\sqrt{2\pi\sigma^2}} \int_{-\infty}^{\infty} \exp\left(-\frac{x^2}{2\sigma^2}\right) \exp(-iqx) dx \\ &= \frac{1}{\sqrt{2\pi\sigma^2}} \int_{-\infty}^{\infty} \exp\left(-\frac{x^2}{2\sigma^2}\right) [\cos(qx) - i \sin(qx)] dx \\ &= \frac{1}{\sqrt{2\pi\sigma^2}} \int_{-\infty}^{\infty} \exp\left(-\frac{x^2}{2\sigma^2}\right) \cos(qx) dx - \frac{i}{\sqrt{2\pi\sigma^2}} \int_{-\infty}^{\infty} \exp\left(-\frac{x^2}{2\sigma^2}\right) \sin(qx) dx \end{aligned}$$

The integral on the right is anti-symmetric around  $x = 0$ , and hence drops out. The integral on the left is not easy to solve, but is given in some more extensive tables of integrals (see e.g. Abramowitz and Stegun (1972), p. 302, equation 7.4.6). This gives,

$$G(q) = \exp\left(-\frac{\sigma^2 q^2}{2}\right)$$

Therefore the Fourier transform of a Gaussian is also a Gaussian with a width, which is the reciprocal of the original width. So the product of two Gaussians in reciprocal space, of reciprocal widths  $\sigma_1$  and  $\sigma_2$  is

$$F(q) = \exp\left(-\frac{(\sigma_1^2 + \sigma_2^2)q^2}{2}\right)$$

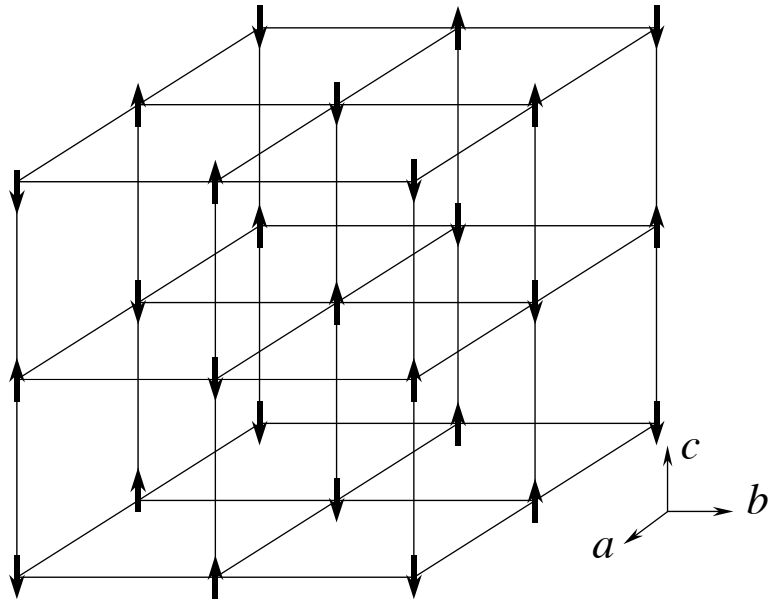
By inspection, the inverse Fourier transform of  $F(q)$  can now be written down, giving

$$f(x) = \frac{1}{\sqrt{2\pi(\sigma_1^2 + \sigma_2^2)}} \exp\left(-\frac{x^2}{2(\sigma_1^2 + \sigma_2^2)}\right)$$

Therefore the convolution of two Gaussians is a Gaussian function, where the widths of each are added in quadrature.

## K2.1

The moments point along  $c$  and each atom is antiferromagnetically coupled to its nearest neighbour, i.e. the magnetic unit cell is twice as large along  $a$ ,  $b$ , and  $c$ :

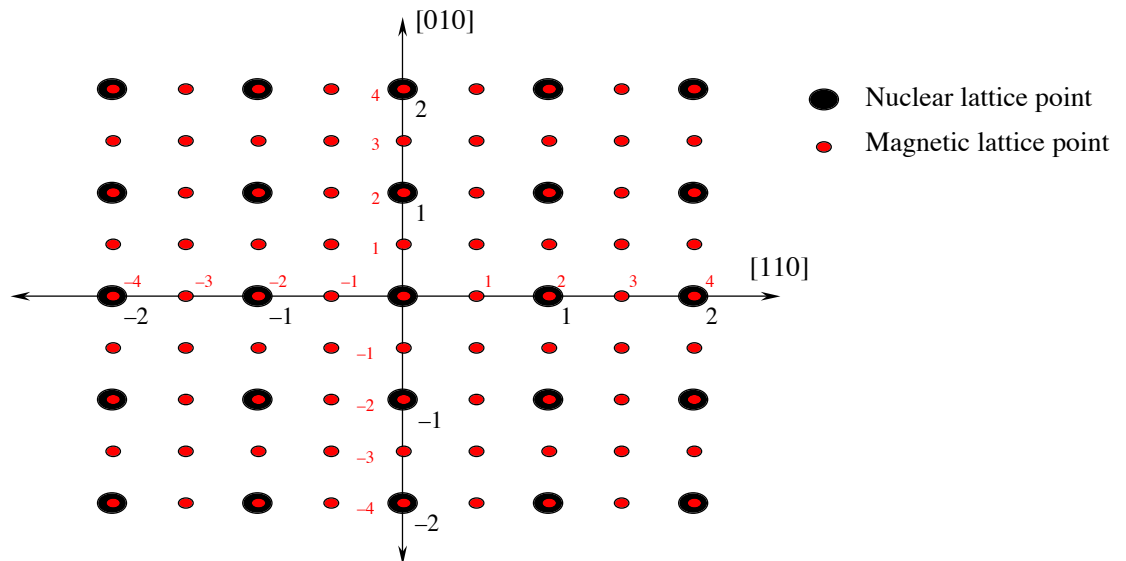


## K2.2

The nuclear unit cell is primitive, thus Bragg peaks will appear at all the points in  $h$ ,  $k$  and  $l$ .

## K2.3

The magnetic unit cell is twice as large as the nuclear in  $a$ ,  $b$  and  $c$ , hence the magnetic reciprocal lattice is half the size of the nuclear reciprocal lattice.



Nuclear indices written in black, magnetic in red.

## K2.4

The magnetic structure factor is given by the Fourier transform of the moment orientations and positions, i.e.

$$F_{mag}^{hkl} = \sum_{j=1}^N \mu_j \exp\left(2\pi i(hx_j + ky_j + lz_j)\right)$$

where  $N$  is the number of moments in the unit cell. There are 8:

Atom	(x,y,z)	Moment amplitude
1	(0, 0, 0)	+1
2	(0.5, 0.5, 0)	+1
3	(0.5, 0, 0.5)	+1
4	(0, 0.5, 0.5)	+1
5	(0.5, 0, 0)	-1
6	(0, 0.5, 0)	-1
7	(0, 0, 0.5)	-1
8	(0.5, 0.5, 0.5)	-1

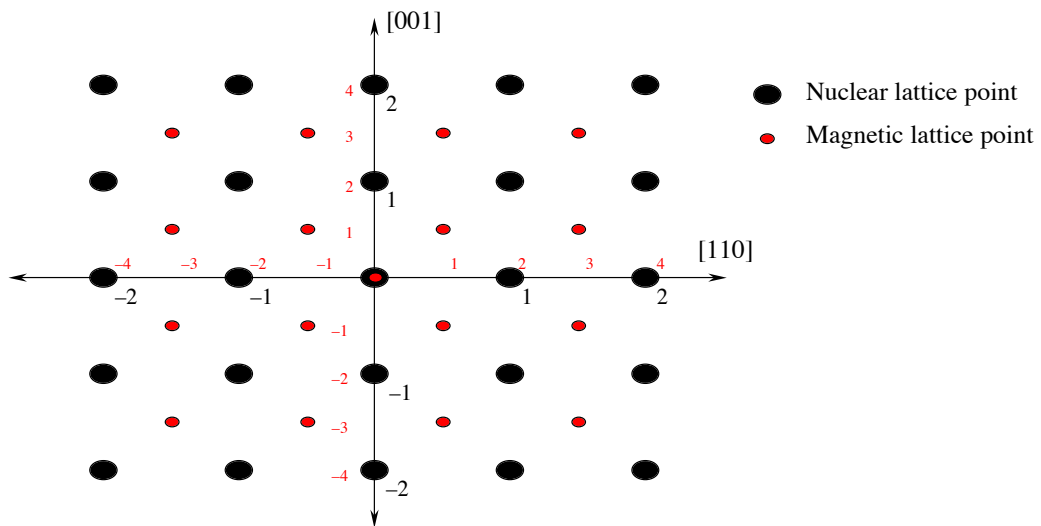
Note that (x,y,z) are defined with respect to the *magnetic* unit cell, and the amplitude is given in units of  $\mu$ .

Substitute these values in to the equation, which becomes:

$$F_{mag}^{hkl} = \mu \begin{pmatrix} 1 + \exp(\pi i(h+k)) + \exp(\pi i(h+l)) + \exp(\pi i(k+l)) \\ -\exp(\pi i h) - \exp(\pi i k) - \exp(\pi i l) - \exp(\pi i(h+k+l)) \end{pmatrix}$$

This equals zero for all  $h,k,l$  except when they are all odd!

The Bragg peak map therefore looks like:



This comes about because the magnetic unit cell has a higher symmetry than the nuclear unit cell. It is, in fact, face-centred cubic with 4 moments in its basis.

The structure factor for all the visible lattice points is  $8\mu$ , however the intensities of the Bragg peaks will *not* be all the same (despite them all having the same structure factor). The direction of  $\mathbf{Q}$  with respect to the moment direction becomes important. Neutrons only ever see the perpendicular component of the sublattice magnetization to  $\mathbf{Q}$ , thus the intensity of the Bragg peaks will be multiplied by  $\sin^2\phi$ , where  $\phi$  is the angle between  $\mathbf{Q}$  and [001].

Furthermore, the intensity will be modulated by the magnetic form factor. This will cause the intensity to *decrease* with *increasing Q*.

### K2.5

The spin waves will be visible in both directions. However, the spin waves in the classical picture take the form of fluctuations that are perpendicular to the mean moment direction. Hence, if the moments are oriented along  $c$ , the spin waves will take the form of fluctuations in the  $(a, b)$  plane. Measurements along the [001] axis will therefore see the full contribution from the spin waves as this direction is normal to the  $(a, b)$  plane, as  $\mathbf{Q}$  is always perpendicular to the moment contributions. Measurements along the [110] axis will only have half this intensity as components of the spin waves along [110] will not give any neutron scattering.

### K2.6

If the sample has many domains, there will be no distinction between moments lying along  $a$ ,  $b$ , or  $c$ . Therefore the  $\sin^2\phi$  term will need to be averaged over all possible orientations, i.e. the magnetic (511) and (333) peaks (which have the same  $Q$ ) will have the same intensity.

## L. Chemical Applications

### **L1.**

#### **(A and B)**

HINT #1: calculate the volume of one water molecule (approx.  $29.9 \text{ \AA}^3 = 29.9 \times 10^{-30} \text{ m}^3$ )? (what is the mass of one mole of water? (18g/mol) What is the volume of one mole of water ( $18 \text{ cm}^3$ )? What is the relative volume of one molecule of  $\text{H}_2\text{O}$  and one of  $\text{D}_2\text{O}$ ? (electrons determine the molecular ‘size’ not the nucleus so they should be approximately equal).

HINT #2: what is the scattering length of one molecule of (a)  $\text{H}_2\text{O}$

$$\{(-3.74*2)+5.803\} * 10^{-15} \text{ m} = -1.677 \times 10^{-15} \text{ m}$$

and (b)  $\text{D}_2\text{O}$ ?

$$\{(+6.671*2)+5.803\} * 10^{-15} \text{ m} = +19.145 \times 10^{-15} \text{ m}$$

Hence find the scattering length densities of  $\text{H}_2\text{O}$  and  $\text{D}_2\text{O}$  (-0.56 and  $6.4 \times 10^{-6} \text{ \AA}^{-2}$ )

Isotope	Scattering length density / ( $\text{\AA}^{-2}$ )	Refractive index calc	Refractive Index
H	$\text{H}_2\text{O} = -0.56 \times 10^{-6}$	$1 + 2.8874 \times 10^{-7}$	1.000000289
D	$\text{D}_2\text{O} = +6.40 \times 10^{-6}$	$1 - 3.289 \times 10^{-6}$	0.99999670
O			
Si	$2.07 \times 10^{-6} \text{ \AA}^{-2}$	$1 - 1.067 \times 10^{-6}$	0.999998933

#### **(C)**

Critical angle is given by:

$$\frac{n_1}{n_0} = \frac{\cos \theta_0}{\cos \theta_1} \quad \text{Where } \theta_0 \text{ and } \theta_1 \text{ are the grazing angles of reflection, or}$$

$$\frac{n_1}{n_0} = \cos \theta_c : \text{D}_2\text{O}/\text{Si} = 0.99999670(\text{D}_2\text{O})/0.999998933 (\text{Si}) = 0.99999776$$

$$= \cos \theta_c$$

$$\rightarrow \theta_c = 0.00211 \text{ radians}$$

$$\rightarrow = 0.121^\circ$$

$$Q = \frac{4\pi i \sin \theta_c}{\lambda} = 4 * \pi i * \frac{\sin \left( 0.121 * \left( \frac{\pi}{180} \right) \right)}{1.8} = 0.01466 \text{ \AA}^{-1}.$$

#### **(D)**

If critical edge is at 0.1 degrees (0.00174 rad): then SLD of the water phase is:

$$n_{\text{water}} / 0.999998933 (\text{Si}) = \cos \theta_c = \cos (0.1) = 0.999998486$$

Refractive index of water is: 0.999997419  $\rightarrow$  SLD = +5.0e-6 Å-2.

Pure H<sub>2</sub>O is:  $-0.56 \times 10^{-6} \text{ Å}^{-2}$

Pure D<sub>2</sub>O is:  $+6.4 \times 10^{-6} \text{ Å}^{-2}$

Difference:  $= 6.96 \times 10^{-6} \text{ Å}^{-2}$

SLD D<sub>2</sub>O – SLD from data is: 1.4  $\rightarrow$  20% H<sub>2</sub>O therefore 80% D<sub>2</sub>O

Hence water is 20% H<sub>2</sub>O and 80% D<sub>2</sub>O.

(Check: SLD:  $-0.11 + 5.1 = 5.0 \times 10^{-6} \text{ Å}^{-2}$ .  $\rightarrow n_{\text{water}} = 0.999997419$ . As required.)

## L2

(a) Incoherent neutron scattering (ONLY) sees the protonated species (octane in this case). As we add more decane we can't see its scattering but we can see the amount of octane on the surface fall as the decane pushes it off.

(b)

$$X_{\text{bulk}} = 1.0; X_{\text{surface}} = 1.0$$

$$X_{\text{bulk}} = 0.909; X_{\text{surface}} = 0.6 \text{ (get a ruler??)}$$

$$X_{\text{bulk}} = 0.715; X_{\text{surface}} = 0.10$$

Graph:

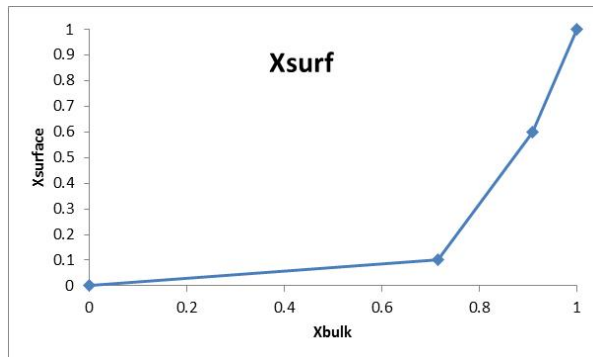


**Figure L1a**

Conclusion: the decane is strongly preferentially adsorbed. It has a much higher surface concentration than the bulk (at any concentration).

\*PkA surface charge.. how much adsorbs at different pH.

## **M. Biological Applications**

### **M1**

A, this question simply involves summing the scattering lengths for the particular molecule using the values given on tables 1 and 2 and then dividing them by the molecular areas given:

$$\text{Sum b tails} = (26 \times 6.646 \times 10^{-5} \text{ \AA}) + (54 \times -3.71 \times 10^{-5} \text{ \AA}) = -28.54 \times 10^{-5} \text{ \AA}$$

$$\rho_{\text{tails}} = -28.54 \times 10^{-5} \text{ \AA} / 771 \text{ \AA}^3 = -0.037 \times 10^{-5} \text{ \AA}^{-2} \text{ or } \underline{-0.37 \times 10^{-6} \text{ \AA}^{-2}}$$

$$\text{Sum b headgroup} = (10 \times 6.646 \times 10^{-5} \text{ \AA}) + (18 \times -3.71 \times 10^{-5} \text{ \AA}) + 9.36 \times 10^{-5} \text{ \AA} + (8 + 5.8 \times 10^{-5} \text{ \AA}) + 5.13 \times 10^{-5} \text{ \AA} = 60.21 \times 10^{-5} \text{ \AA}$$

$$\rho_{\text{headgroup}} = 60.21 \times 10^{-5} \text{ \AA} / 304 \text{ \AA}^3 = 0.198 \times 10^{-5} \text{ \AA}^{-2} \text{ or } \underline{1.98 \times 10^{-6} \text{ \AA}^{-2}}$$

These values can then be used to determine lipid coverage in question 2.

### **M2**

A, There is a significant difference in  $\rho$  between the lipid headgroup ( $1.98 \times 10^{-6} \text{ \AA}^{-2}$ ) and  $\text{H}_2\text{O}$  ( $-0.56 \times 10^{-6} \text{ \AA}^{-2}$ ), but no real difference between the tails ( $-0.37 \times 10^{-6} \text{ \AA}^{-2}$ ) and  $\text{H}_2\text{O}$ . Both bilayer components have contrast in the  $\text{D}_2\text{O}$  ( $6.35 \times 10^{-6} \text{ \AA}^{-2}$ ) solution but the tails have the most significant difference. Therefore the answer is:

Tails in  $\text{D}_2\text{O}$  and headgroups in  $\text{H}_2\text{O}$ . However students should be commended for noting that in  $\text{D}_2\text{O}$  both headgroups and tails have contrast with the solution.

B, from the lectures students should be familiar with the SLD profile of a bilayer across the solid/liquid interface. The layers relate to the interfacial components are follows:

**Layer 1 : Silicon oxide**

**Layer 2, Inner bilayer headgroups**

**Layer 3, bilayer tails**

**Layer 4, outer bilayer headgroups**

C, from **M2.A**, it should be determined that the  $\text{D}_2\text{O}$  contrast was especially sensitive to the lipid tails due to a large difference in  $\rho$  between the tails and the solution in this contrast. From **M2.B**, layer 3 in the 4 layer model should have been identified as the lipid tails (with a fitted  $\rho$  in the  $\text{D}_2\text{O}$  contrast of  $0.17 \times 10^{-6} \text{ \AA}^{-2}$ )

The values required to determine the volume fraction ( $\phi$ ) of the lipid at the solid liquid interface are therefore:

$$\rho_{\text{fitted}} = 0.17 \times 10^{-6} \text{ \AA}^{-2}$$

$$\rho_{\text{tails}} = -0.37 \times 10^{-6} \text{ \AA}^{-2}$$

$$\rho_{\text{D}_2\text{O}} = 6.35 \times 10^{-6} \text{ \AA}^{-2}$$

To determine  $\phi_{\text{tails}}$  you can use:

$$\phi_{\text{tails}} = \frac{(\rho_{\text{D}_2\text{O}} - \rho_{\text{fitted}})}{(\rho_{\text{D}_2\text{O}} - \rho_{\text{tails}})}$$

Resulting in:

$$\varphi_{tails} = \frac{(6.35 - 0.17)}{(6.35 - -0.37)}$$

Which gives  $\varphi_{tails} = 0.92$ , a 92% coverage of the interface with the lipid bilayer.

### M3

A,  $7.45 \times 10^{-6} \text{ \AA}^{-2}$ , the calculation used was the same as in 1, A.

B, as the only difference between the SLD of the tail layers in D<sub>2</sub>O and H<sub>2</sub>O is due to the presence of the water you can determine the water content by:

$$\varphi_{water} = \frac{(\rho_{fitted,D2O} - \rho_{fitted,H2O})}{(\rho_{D2O} - \rho_{H2O})}$$

This gives the following answer for the inner leaflet:

$$\varphi_{water \ inner \ tails} = \frac{(6.06 - 5.71)}{(6.35 - -0.56)} = 0.05$$

And the following answer for the outer leaflet:

$$\varphi_{water \ outer \ tails} = \frac{(0.95 - 0.61)}{(6.35 - -0.56)} = 0.05$$

Both leaflets contain 5% hydration and therefore a bilayer coverage of 95% ( $\varphi_{lipid} = 0.95$ ) is found.

C, this equation can be done a number of ways but essentially it comprises comparing the fitted  $\rho$  value from either the H<sub>2</sub>O or D<sub>2</sub>O contrast to the known  $\rho$ 's of the deuterated and hydrogenated lipid. The way I did it involved calculating the  $\varphi_{DPPC}$  and as the  $\varphi_{water}$  is known the  $\varphi_{LPS}$  is simply 1- ( $\varphi_{DPPC} + \varphi_{water}$ ):

$$\varphi_{DPPC} = \varphi_{lipid} \times \left( \frac{((\rho_{fitted} - (\rho_{D2O} \varphi_{D2O}) / \varphi_{lipid}) - \rho_{h-lipid \ tails})}{(\rho_{d-lipid \ tails} - \rho_{h-lipid \ tails})} \right)$$

This gives the following answer for the inner leaflet:

$$\begin{aligned} \varphi_{DPPC} &= 0.95 \times \left( \frac{(((6.06 - (6.35 \times 0.05) / 0.95) / 0.95) - -0.37)}{(7.45 - -0.37)} \right) \\ &= 0.78 \end{aligned}$$

As  $\varphi_{DPPC} = 0.78$  and  $\varphi_{water} = 0.05$ ,  $\varphi_{LPS} = 0.17$  (by 1- ( $\varphi_{DPPC} + \varphi_{water}$ ) for the inner leaflet.

For the outer leaflet:

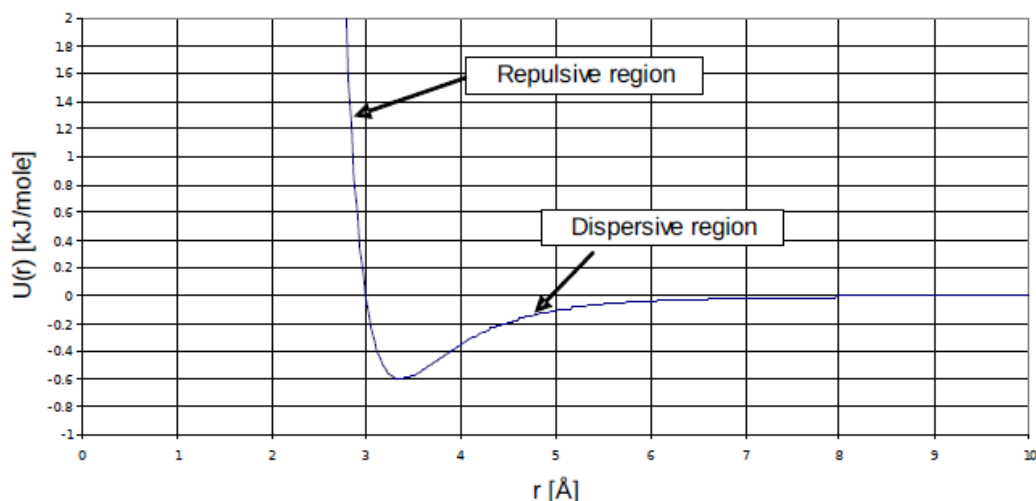
$$\begin{aligned} \varphi_{DPPC} &= 0.95 \times \left( \frac{(((0.95 - (6.35 \times 0.05) / 0.95) / 0.95) - -0.37)}{(7.45 - -0.37)} \right) \\ &= 0.13 \end{aligned}$$

As  $\varphi_{DPPC} = 0.13$  and  $\varphi_{water} = 0.05$ ,  $\varphi_{LPS} = 0.82$  (by 1- ( $\varphi_{DPPC} + \varphi_{water}$ ) for the outer leaflet.

## N. Disordered Materials Diffraction

**N1.1 a) and c)**

**Lennard-Jones potential**

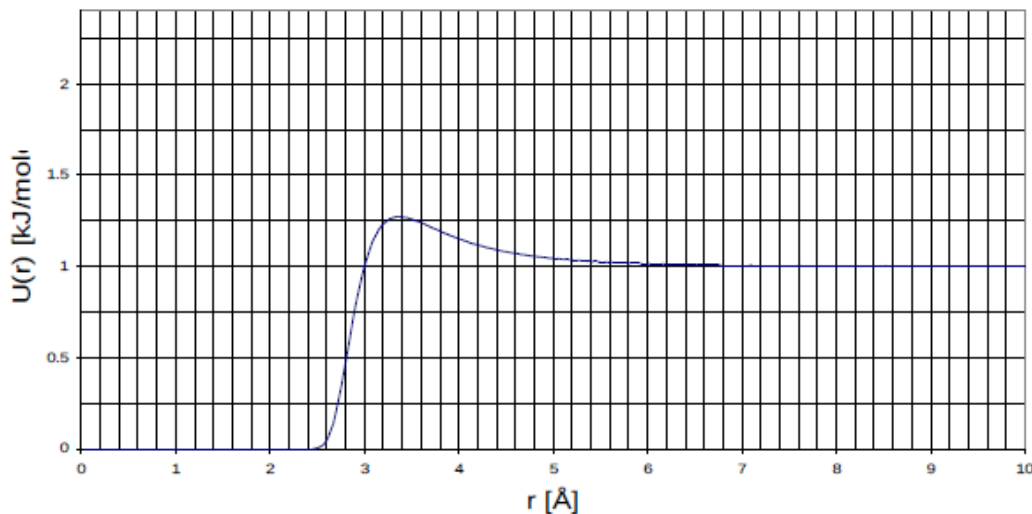


**N1.1 b)**

$\epsilon$  represents the depth of the potential. It controls how tightly adjacent atoms are bound.  $\sigma$  represents the radius at which the hard core repulsive region goes to zero. It represents roughly the distance of closest approach of two atoms.

**N1.2 a)**

**Lennard-Jones gas  $g(r)$  at 300K**



**N1.2b)**

At low  $r$ ,  $U(r)$  becomes very large, while  $g(r)$  goes to zero. At high  $r$ ,  $U(r)$  goes to zero, while  $g(r)$  goes to unity. In between the two functions are in rough antiphase.

**N1.2c)** If  $\epsilon$  were increased by a factor of 2, the height of the peak in  $g(r)$  at  $\sim 3.8\text{\AA}$  would grow from  $\sim 1.27$  to  $\sim 1.54$ . If  $\sigma$  were increased by 20%, the main peak would move out by 20%, but would remain the same height.

**N1.3a)**

In the gas form  $g(r)$  decays monotonically to unity at large  $r$ . As the density increases the height of the main peak increases and it becomes sharper as a series of decaying oscillations occur towards larger  $r$ . All the peaks move to smaller  $r$  with increasing density.

Based on a change of density of 0.02 to 0.035, one might expect the separation of peaks to change by the cube root of the ratio of densities, namely

$$\sqrt[3]{0.02 / 0.035} = 0.83$$

In fact the first peak moves from  $3.18\text{\AA}$  to  $3.06\text{\AA}$ , a fractional change of only 0.96, while the second peak moves from  $6.39\text{\AA}$  to  $5.91\text{\AA}$ , a fractional change of 0.92. In other words the peaks in  $g(r)$  do NOT represent the mean separation of the atoms. This can be quite confusing!

**N1.3b)**

Fundamentally as the material becomes more dense the direct interactions between atoms 1 and 2 become increasingly affected by the presence of 3rd, 4th , etc. atoms which increasingly surround them, and which increasingly confine them in space. Within the pairwise additive approximation assumed here all the atoms interact via known pairwise forces, but the result is many body correlations which are difficult to predict accurately. A raft of theoretical methods to do this approximately exist, but few if any of them work for the kind of interatomic forces that are found in real materials. Hence in practice one has little option but to use computer simulation to determine the effect of many-body correlations in real materials. This problem affects crystals as much as it affects liquids, but in a crystal one has a repeat lattice (which is itself a consequence of many body correlations) which we can determine from the position and height of the Bragg peaks. In any case the primary goal of interest in crystallography is the single particle correlation function (the lattice),

not the higher order correlations. The single particle correlation function for a liquid is uniform and contains no information. For a glass it is not uniform, but contains no repeat distances.

#### N1.4a)

For density 0.02 the first minimum occurs at  $4.95\text{\AA}$ , giving a coordination number of  $\sim 10$  atoms. For density 0.035, the first minimum is at  $4.47\text{\AA}$  with a coordination number of 12.5. Clearly these numbers do not scale with density change: coordination number varies less rapidly than the density.

#### N1.4b)

If instead we had used the same radius,  $4.47\text{\AA}$ , then the coordination number at density 0.02 is 7.23, a ratio of 0.58 compared to density 0.035, which is quite close to the ratio of densities, 0.57. This illustrates again that peaks and dips in  $g(r)$  do not correlate directly with the density, although they are obviously related to it.

#### N1.5a)

The primary effect of changing the density on the structure factor is to increase the amplitude of the oscillations. There is some movement of the peaks as well, but fundamentally as the density increases they become sharper, and the oscillations extend to large  $Q$ .

#### N1.5b)

For density 0.02, the first peak in  $g(r)$  is at  $3.18\text{\AA}$  and the first peak in  $S(Q)$  is at  $2.2\text{\AA}^{-1}$ . For density 0.035, the first peak in  $g(r)$  is at  $3.06\text{\AA}$  and the first peak in  $S(Q)$  is at  $2.35\text{\AA}^{-1}$ , i.e. as the peaks in  $g(r)$  move in, those in  $S(Q)$  move out, although the movement of the first peak in  $S(Q)$  is more related to the movement of the 2nd and subsequent peaks in  $g(r)$  than it is to the first peak in  $g(r)$ .

#### N1.5c)

It depends how we did it. If we increased  $\sigma$  at constant density, then the peaks would move out, but also become markedly sharper as the packing fraction of the liquid increased. If the density was reduced to compensate for the increase (atoms occupying more space) then the peaks in  $S(Q)$  would move in, but without increased amplitude.

#### N1.5d)

Since the structure factor only exists if the density is finite, a zero density will produce zero structure factor.

**N2.1a)**

Atomic fractions are  $c_{\text{Zn}} = 1/3 = 0.333$ ,  $c_{\text{Cl}} = 2/3 = 0.667$

**N2.1b)**

$$F(Q) = \frac{1}{9} b_{\text{Zn}}^2 H_{\text{ZnZn}}(Q) + \frac{4}{9} b_{\text{Zn}} b_{\text{Cl}} H_{\text{ZnCl}}(Q) + \frac{4}{9} b_{\text{Cl}}^2 H_{\text{ClCl}}(Q)$$

**N2.1c)**

In essence the idea is that we measure  $F(Q)$  for three samples, namely one with only  $^{35}\text{Cl}$  isotope present, another with only  $^{37}\text{Cl}$  isotope present, and a third with a mixture of  $x$  parts  $^{35}\text{Cl}$  and  $(1-x)$  parts of  $^{37}\text{Cl}$ . For this third sample the chlorine scattering length is

$$b_{\text{mix}} = x b_{^{35}\text{Cl}} + (1-x) b_{^{37}\text{Cl}}$$

which means the weighting coefficient of the  $H_{\text{ClCl}}$  partial structure factor for this sample is not a linear combination of the same coefficient for the other two samples. This means the determinant of coefficients in the above formula for the three samples is finite and the matrix of coefficients can be inverted. Hence the three measurements can be used to extract the three partial structure factors, at least in principle.

A basic assumption of the isotope substitution method is that the partial structure factors do not change appreciably with isotopic composition of the sample. This is an accurate assumption in most cases, but is less accurate when hydrogen is replaced with deuterium, particularly at low temperatures and with larger molecules, because in these cases quantum effects due to the different masses can impact on both the structure and the phase diagram of the material in question.

**N2.1d)**

Remarkably few in practice. There have been attempts to perform isomorphic substitution with X-rays, but these method tends to be shrouded in uncertainties from knowing whether one atom can substitute for another without . Then there has been the combination of neutrons, X-rays and electrons, but each technique requires quite different sample containment, making comparisons of the three results dubious. A more promising approach is the use of anomalous dispersion of Xrays, whereby you vary the scattering length of one component near an absorption edge. This method is quite promising, but requires highly stable precision equipment to be performed satisfactorily, and to date has only be tried on a handful of materials. It suffers also from poor counting statistics because of the high degree of monochromatisation needed for the incident beam of X-rays.

Recently we have been exploring the use EXAFS to refine liquid and glass structures, and this approach looks very promising indeed.

### N2.2a)

This is a very common problem in neutron scattering using isotopes: one or more of the components makes only a small contribution to the scattering pattern. In this case it is the ZnZn structure factor. Below is shown the inversion of the weights matrix:-

**Table N2a:** *Inversion of the matrix coefficients of Table N1*

Partial Structure Factor	Zn <sup>35</sup> Cl <sub>2</sub>	Zn <sup>mix</sup> Cl <sub>2</sub>	Zn <sup>37</sup> Cl <sub>2</sub>
Zn-Zn	37.25	-71.53	62.16
Zn-Cl	-21.87	39.37	-17.50
Cl-Cl	10.15	-14.99	4.84

You will notice that to extract the ZnZn partial structure factor we need to multiply the data by large numbers and then add and subtract them, making us rely heavily on the absolute accuracy of the diffraction data if we are to avoid amplifying systematic data errors in the final structure factor.

Obtaining absolute scattering cross sections with accuracies better than 1% is a tall order with any technique, including neutrons, and is rarely achieved.

### N2.2b)

Particular difficulties are:-

- a) The data are only available over a finite Q range;
- b) The data are multiplied by Q in the integrand of (1.5) making the effect of statistical uncertainty at high Q a particular difficulty.
- c) No matter how careful they are measured and corrected, diffraction data always have systematic errors, which can seriously perturb the Fourier transform, particularly at low r.

Fourier transform of data with potential significant systematic error is risky: the systematic error can have the effect of introducing marked backgrounds in real space that can make the peaks larger or smaller than they should be. As a consequence coordination numbers can be faulty when extracted by this method.

### N2.2c)

Fourier transforms of raw data should be avoided whenever possible. Instead the data should be compared with a structural model of the data, and then, assuming the model is satisfactory, use the model to generate the real space distributions, as well as address other questions about the structure of the material. Computer simulation is a convenient method to produce such a structural model of the measured scattering cross sections. This model will also help to identify what might be wrong (if there is anything) with the data, and avoid some of the problems introduced by systematic effects. Some authorities are reluctant to use computer simulation to achieve this, since it too can introduce systematic bias in the interpretation of the data, and so instead invoke a series of consistency checks on the data. These are used to identify and correct particular problems with the data, but this can be a very time consuming process which can take months to resolve. The net effect is the same however: in computer simulation one is already applying a series of physical consistency checks on the data, with the advantage that you have at the end a physical model of the scattering system which is consistent with your scattering data. With the other methods, you have corrected data, but you still have the problem of trying to understand what they mean.

### N2.3a)

Figure G2.2 shows the running coordination number of this  $g(r)$ . From this graph we can read that at the first minimum,  $3.4\text{\AA}$ , the running coordination number is  $\sim 4.3$  Cl about Zn. Since there are half the number Zn atoms compared to Cl, the coordination number of Zn about Cl will be 2.2.

### N2.3b)

The first ZnCl peak is at  $2.31\text{\AA}$ , while the first ClCl distance is at  $3.69\text{\AA}$ . Using the cosine rule, I estimate the Cl-Zn-Cl angle to be  $106^\circ$ , which is close to the tetrahedral angle of  $109.47^\circ$ . This together with the coordination number of  $\sim 4$  is a strong hint of likely tetrahedral local coordination in this liquid.

Taking this argument a bit further, one notices that the first ZnZn peak is at  $3.93\text{\AA}$ , while the second is at  $6.81\text{\AA}$ , giving a Zn-Zn-Zn angle of  $120^\circ$ , suggesting also that at least the Zn packing is not simple, and probably maps into the roughly tetrahedral packing of the Cl around Zn, with significant edge-sharing of the tetrahedra.

### N2.3c)

Looking at the curves one is struck by the way the ZnCl oscillations are almost exactly out of phase with the ZnZn and ClCl oscillations. This behaviour strongly indicative of charge ordering, although it is not entirely clear that Zn and Cl are fully ionic in this system.